FLOW AND FRACTURE IN SPINEL STRUCTURED CERAMICS

Contract No. DA-31-124-ARO-D-207
Department of Army Project No. 2001050113700

Hayne Palmour III
Chief Investigator

SECOND TECHNICAL REPORT

"FLOW AND FRACTURE OF HOT-PRESSED POLYCRYSTALLINE SPINEL AT ELEVATED TEMPERATURES"

by

Dong M. Choi and Hayne Palmour III

July, 1965

Department of Engineering Research
North Carolina State University at Raleigh

Flow and Fracture of Hot-Pressed Polycrystalline Spinel at Elevated Temperatures*

by

Dong Myung Choi and Hayne Palmour III

ABSTRACT

High purity (approximately 99.94%) fine particle size (40 m) $MgAl_2O_4$ spinel prepared by chemical coprecipitation was hot pressed using the rate-controlled method in a graphite die. The average density of three hot-pressed compacts was 99.2% of theoretical and the average grain size was 0.5μ. Compression specimens cut from these compacts were heat treated at various temperatures and time periods to achieve the desired amount of grain growth.

The specimens then were tested in compression in vacuo at prescribed temperatures and strain rates and the amount of flow stress (the dependent variable in this investigation) was measured in each case. Grain size, temperature, and strain rate (the independent variables in this investigation) covered the range 0.5 - 200μ,

---

*Based upon a dissertation submitted by Mr. Choi in partial fulfillment of the requirements for the Degree of Doctor of Philosophy.

1350 - 1800°C, and 0.05 - 5%/min, respectively.

Utilizing an IBM-1410 computer for data reduction and statistical analysis, the correlations between the indendent variables were established. The microstructure of specimens was examined carefully after the test and the findings were related to the work hardening revealed in the stress-strain diagrams and to the failure mechanism of the specimens.

Hot-pressed spinel deforms plastically within the experimental ranges of this investigation. The stress at which plastic flow initiates depends largely on the temperature and to a lesser extent on the strain rate and grain size. The maximum average flow stress of hot-pressed spinel was approximately 42,000 psi for the specimen with 10μ grain size tested at 0.5%/min strain rate and at a temperature of 1350°C. Work hardening is consistently observed in the stress-strain diagrams obtained in this investigation and the degree of work hardening is shown to be strongly dependent on the strain rate, temperature, and grain size. Wavy slip lines and recrystallization in specimens with intermediate grain sizes are indicative of plastic deformation involving dislocation movements along multiple slip planes.

ACKNOWLEDGMENTS

The authors gratefully acknowledge many encouraging and fruitful discussions with Doctors W. W. Kriegel, R. F. Stoops, W. C. Hackler, H. H. Stadelmaier, R. R. Patty, J. V. Hamme, and A. H. E. Grandage of the N. C. State University faculty. Dr. A. E. Lucier, M. L. Huckabee, D. E. Witter, L. J. Ferrell, and H. Z. Dokuzoguz provided valuable assistance in the experimental phases of the research.

TABLE OF CONTENTS

LIST OF TABLES

LIST OF ILLUSTRATIONS

LIST OF ILLUSTRATIONS (continued)

INTRODUCTION

Ceramic materials are, in general, economical, readily available, hard, and resistant to corrosion by oxidizing elements. The oxides such as alumina, magnesia, spinel, and zirconia have high melting temperatures and are structurally stable even near their melting points. Nevertheless, until recent decades, metals have been the material of choice for structural members because of the characteristic brittleness of typical ceramics. Application of a sudden external stress causes most ceramic materials to shatter whereas metals undergo a considerable amount of plastic deformation before failing.

However, with the rapid expansion in modern technologies now underway, a structural component is required which has the advantageous properties of both metals and ceramics. At present no single material is known to have this unique combination of properties. The search for this material will become more effective as the underlying reasons for ceramics' brittleness and metals' ductility become better understood.

On the basis of calculated bonding forces, metals should have far greater theoretical strength than the strength that is actually observed in them. The low strength of metals results from movements of dislocations on certain crystallographic planes along specific directions under the applied shear force. This movement of dislocations induces plastic deformation in metals at a much lower stress level than is

expected from classical theory. However, dislocations in most ceramic materials are relatively immobile at room temperature, partly because of the large lattice energy barrier and partly because of the complex crystalline structure. Consequently, most ceramics exhibit very little or no ductility at all. At elevated temperatures, dislocations in normally brittle ceramic materials become mobile, thus imparting plasticity. Even so, most refractory ceramics are ductile only to a small extent because of the limited mobility of their dislocations on the limited number of available slip systems.

Spinel ($MgAl_2O_4$) melts at a high temperature and is chemically inert. Its crystallographic structure is face-centered cubic with close-packed oxygen ions. Spinel does have the multiple slip systems that are necessary for generalized plastic deformations to occur in a polycrystalline body. Because of its structure and bonding, spinel is corrosion resistant, refractory, and thermodynamically stable at high temperatures. The possibility that it may also be ductile at high temperatures is the basis for this research which investigates the deformation in compression of hot-pressed polycrystalline spinel as it depends upon 1) the strain rate or speed at which the material is stressed, 2) the temperature, and 3) the grain size of the body.

REVIEW OF LITERATURE

The experiments reported here deal with the mechanical properties of hot-pressed spinel ($MgAl_2O_4$) at elevated temperatures. The strength of a polycrystalline material depends largely upon its microstructure (e.g., the size, shape, and distribution of the grains and pores). These microstructural features are the direct consequence of the starting materials and of the process by which densification was achieved. The general theories concerning sintering are thus the first topic reviewed.

Sintering

There are two methods of sintering: 1) solid-state sintering and 2) sintering in the presence of a viscous liquid. In both processes, the mechanically and/or chemically bound powders change their size and shape under the appropriate temperature and time conditions, producing a dense body. The driving force for the densification is the decrease in surface area and the reduction in surface-free energy of the grains through the elimination of solid-vapor interfaces. Since liquid-phase sintering is used almost exclusively for firing silicates containing viscous phases or metal bonded cermet systems and since the sintering process involved in the hot pressing of spinel is of the solid-state type, this review will deal with solid-state sintering.

The densification of a powdered material is accompanied by pore removal and, in general, grain growth. During the early stages of solid-state sintering, open pores disappear (Clark and White, 1950) and shrinkage occurs through a neck growth process (Kuczynski et al., 1959). According to the latter there are three possible mechanisms by which neck growth can occur: 1) viscous or plastic flow of microscopic or macroscopic particles, 2) evaporation of ions (or atoms) from convex portions of the system and condensation of these ions in cavities, and 3) bulk and surface diffusion of atoms, ions, and/or vacancies. Their experiments with sapphire spheres showed volume diffusion to be the rate-controlling mechanism. A similar experiment by Coble (1959) with sapphire spheres supports the Kingery-Berg (1955) model of sintering. In this model the neck is identified as the source for vacancies while the contact boundaries (grain boundaries) of the crystals act as vacancy sinks. Thus sintering and shrinkage by neck growth is thought to be controlled by a bulk diffusion process involving vacancy migration.

Sintering studies of polycrystalline Al_2O_3 by Burke (1957) showed that the grain boundaries are apparently good vacancy sinks. A large amount of porosity still remained within the grains while near the boundaries the pores were absent. This preferential removal of porosity along the grain boundaries suggests that, in order to obtain a pore-free dense body, rapid grain growth must be avoided. The

further the pores become isolated from the boundaries, the more difficult it becomes to remove the trapped pores within the grains. The only way that this porosity can be eliminated is by the slow vacancy diffusion process.

Formation of Spinel

Spinel is found in nature in a nearly perfect stoichiometric state, probably formed under pressure in a hydrothermal environment. Anderson (1952) reports that materials with a spinel-type structure were synthesized as early as 1850. Wagner (1936) found that spinels are initially formed at temperatures above 900°C on contact surfaces of two constituent oxides by the reaction $AO + B_2O_3 \rightarrow AB_2O_4$. He states that spinel formation thereafter occurs by the diffusion of cations A^{++} and B^{+++} in opposite directions through the spinel layer previously formed. In this ionic diffusion process, oxygen ions are virtually immobile. Carter (1961) later confirmed this cationic diffusion process for spinel formation by means of the inert marker method.

When single crystals of MgO and Al_2O_3 were fired together in air at 1560°C for 250 hours (Fuerstenau *et al.*, 1961), spinel formed at the contact interface. In these studies it was observed that the thickness of the spinel layer adjacent to Al_2O_3 was ten times greater than that next to MgO. This, they concluded, is an indication of the more rapid diffusion rate of Mg^{++} ions than of Al^{+++} ions through the spinel layer. Navias (1961) has demonstrated that in a

hydrogen atmosphere spinel is formed around both single and polycrystalline alumina at temperatures of 1500 - 1900°C by the vapor diffusion process. Gaseous-phase magnesium oxide was deposited uniformly on the surface of Al_2O_3. In an oxidizing atmosphere, however, spinel formed only at the contact area.

Rankin and Merwin (1916) originally studied the phase relationships in the MgO - Al_2O_3 system, showing $MgAl_2O_4$ as a congruently melting compound at 2135°C. In this work it was found that $MgAl_2O_4$ formed nearly a complete solid solution with α-Al_2O_3. Later Roy *et al.* (1953) confirmed these earlier findings; they reported the maximum solid solution as 86 mol % Al_2O_3(94 wt. %). Recently, Alper *et al.* (1962) reported a maximum solid solution of 11 mol % MgO in $MgAl_2O_4$.

Structure of Spinel

Bragg (1915) studied the structure of spinel by X-ray diffraction. The ideal structure of spinel is one of a face-centered cubic close packing of oxygen ions with cations occupying some, but not all, of the interstitial positions. There are eight $MgAl_2O_4$ molecules in a unit cell of spinel. Metal ions are distributed in the cell so that eight divalent ions occupy eight of sixty-four available tetrahedral sites and sixteen trivalent ions occupy sixteen of thirty-two available octahedral sites. Materials with this type of ionic arrangement are called normal spinels. Bacon (1952) has shown that magnesium aluminate spinel is of this type. Spinels

with trivalent metal ions occupying tetrahedral sites are called "inverse", examples being $NiAl_2O_4$, $MnAl_2O_4$, and $CoAl_2O_4$. Bacon has further shown that the actual structure of magnesium aluminate spinel is very close to the ideal one.

Some Reported Thermal and Mechanical Properties of Spinel

Data on the structural, physical, thermal, electrical, optical, and mechanical properties of spinel as reported in the literature have been compiled by Palmour et al. (1963 b). Spinel has a melting temperature of 2135°C, a theoretical density of 3.60 g/cc, a thermal expansion coefficient of 7.9×10^{-6} $^{\circ}C^{-1}$ at 25 - 1350°C (Anderson, 1952), a thermal conductivity of 0.0159 cal/(sec)(cm^2)($^{\circ}$c/cm) at 800°C (Kingery et al., 1954), and a specific heat of 0.2 cal/g/°c at room temperature (Archibald and Smith, 1953). Its Moh's hardness is 8. Hot-pressed spinel of high density (99+% theoretical), fine grain size (average 5μ) and high purity (99.9+%) has an ultimate compressive strength of 392,000 psi and transverse strength of 33,400 psi at room temperature (Choi et al., 1962). Sintered spinel of lower density (Ryschkewitch, 1941 a, b) has ultimate room temperature compressive and transverse strengths of 270,000 psi and 19,200 psi respectively. The room temperature transverse strength for sintered spinel (approximately 98% theoretical density) is 12,300 psi (Anderson, 1952). The ultimate compressive strength at a temperature of 1400°C is 21,400 psi for sintered spinel

(Kyschkewitch, 1941a) and 79,000 psi (strain rate of 0.02 in/min) for hot-pressed spinel (Palmour and Choi, 1963).

Dislocation and Twinning in Spinel

The dislocation model in spinel was first proposed by Hornstra (1960) and later verified (Hornstra, 1963) by transmission electron microscopy. It is described in terms of four $\langle 112 \rangle$ quarter-partial dislocation on the $\{111\}$ slip planes with total Burgers vectors along $\langle 110 \rangle$ directions. There are a total of twelve possible slip systems in a unit cell of spinel according to this model. Experimentally, dislocation etch pits have been observed in spinel single crystals (McBrayer et al., 1963). The spinel structure is well known for its (111) twinning. The term spinel twinning is used widely in mineralogy to describe a specific type of twinning. Many minerals conform to the spinel twinning law (Kraus et al., 1959).

Hot Pressing

Hot pressing (or pressure sintering) as a forming method has been used widely in the powder metallurgical field. The apparent advantages of hot-pressing over the conventional dry pressing and sintering are that it reduces processing time and that it has a potential in forming dense, fine grained ceramic ware for improved mechanical strength. Thomas and Jones (1960) described the advantages of hot pressing as well as the general principles involved in forming ware by hot pressing.

Because of the nature of the forming method, the mechanisms by which compaction takes place in hot pressing are expected to be somewhat different from free body sintering. The externally applied stress in hot pressing is much larger than the surface energy which provides the driving force in sintering, and significantly enhances the rate of pore removal, thus accelerating the sintering rate at a given temperature. The techniques of hot pressing and the current theories concerning the mechanism of densification during hot pressing are discussed by Jackson (1961). Densification processes of alumina and magnesia were studied in relation to the microstructure developed during hot pressing (Vasilos and Spriggs, 1963). The dielectric and magnetic properties of lead-zirconate-titanate compounds were related to the physical properties resulting from the various hot pressing conditions (Haertling, 1964). In this study it was noted that the electric properties of the hot pressed material improved over those of the body prepared by the conventional sintering technique. Crandall *et al.*, (1961), King (1961) and Mangsen *et al.*, (1960) have investigated the physical and mechanical properties of polycrystalline Al_2O_3 formed by the hot-pressing method. Studies of the effects of grain size on mechanical properties in hot-pressed MgO by Spriggs *et al.* (1964a, 1964b) showed that with increasing grain size the transverse strength increased. Choi *et al.* (1962) have investigated the dependence of room temperature transverse

strength of hot-pressed spinel on its hot-pressing conditions. Kriegel et al. (1964) showed that the increase of total purity in hot-pressed spinel from 99.5% to 99.9% increased the ultimate compressive strength by approximately ten fold (20,000 psi) at 1600°C.

Strength of Crystalline Solids

The strength of a crystalline material is the measure of the force with which it just resists an externally applied stress. Theoretically this strength is based upon the attractive forces of atoms or ions that are present in the crystal. Thus crystals with different atomic compositions differ in strength. Actually, however, strength depends in part on many other factors, e.g., disturbances in the atomic arrangement, faults in the surface of the crystal, etc. These are called crystalline and surface defects. One of the most important defects is the now well known dislocation. Through dislocation concepts, it is possible to understand many of the complex mechanical responses of crystalline solids, e.g., ductility and strain (work) hardening. Specimens of normally brittle magnesium oxide single crystals, when prepared properly, were plastically deformable at room temperature (Parker, 1961). At elevated temperatures single crystal aluminum oxide was shown to be plastic (Watchman and Maxwell, 1954, 1957; Kronberg, 1955, 1957; May, 1959; Gibbs, 1959; and Conrad, 1965). Ductility in these crystals was clearly attributed to moving dislocations.

The properties of dislocations in crystalline ceramic material are quantitatively quite different from those in metals. Generally ceramic materials have two or more ionic species differing in size and related by short-range, directed bonding forces. In addition their structure normally is more complex than that of metals. When dislocations move in a ceramic material, bonds, ionic and covalent, must be broken and the overall electrostatic neutrality of the lattice must be restored after the reestablishment of the bonds. This process takes place with a low lattice energy involvement in metals, whereas in most ceramic materials high thermal activation is necessary to achieve sufficient mobility for dislocation motion.

Thus by means of dislocation theory the strength of crystalline material can be explained and understood rather well. However, entirely elastic theories must be invoked in coping with the low strength of brittle materials in which dislocations either do not exist, e.g., in glass, or are immobile at a given temperature. Early in the 1920's, Joffe et al. (1924) learned that when a NaCl crystal is dipped in water the brittleness disappears with an increase in strength. This phenomenon was explained through the concept of the surface microcrack. The microcracks in the surface of the crystal act as fracture initiation points causing premature brittle fractures at stress levels far below theoretical strength. The microcrack idea for brittle failure of a crystal was expressed mathematically by

Griffith (1921) on the basis of surface energy:

$$R = \frac{2E\alpha}{\pi\nu C}^{\frac{1}{2}} \qquad ---(1)$$

where R = plane stress or fracture stress

E = Young's modulus

α = surface energy of crystal

ν = Poisson's ratio

C = length of microcrack on the crystal surface

Strengths predicted by this equation were experimentally substantiated with thin glass plates.

Gorum *et al*. (1958) found that embrittlement of ionic crystals (NaCl, KCl) is caused by surface dislocation pile-ups which produce internal stress. Such pile-ups intensify the stress in unslipped portions of the crystal ahead of the advancing columns of dislocations to levels much higher than the applied stress. Consequently, fracture initiates at the surface of the crystal. According to Stroh (1954) cleavage cracks form as a result of dislocation pile-up when:

$$n\sigma \geq 12\ h\ G \qquad ---(2)$$

where n = number of positive dislocations

σ = tensile stress

h = material constant

G = rigidity modulus

He estimated from this equation that the number of dislocations necessary to cause the failure of copper by the pile-up process is approximately 1000. Westwood (1961) and Johnston *et al*. (1961) demonstrated that the pile-up of edge dislocation (from a single slip band) in the grain boundary of

magnesium oxide bi-crystals caused transgranular or intergranular cracks depending on the degree of misorientation between the crystals. Crack formation by the same process (Zener, 1948) was further evidenced in the experiment by Clark *et al*. (1962) with MgO bi-crystals.

It is known that strength in crystalline material is a structure-sensitive property. As mentioned, internal stress in a crystal affects its strength and in the case of a polycrystalline body, its effects on strength become even more significant, as Coble (1958) describes in a comprehensive treatise on the subject. Stokes (1963) has summarized and interpreted the data that has been accumulated primarily since 1958 regarding this. Ryschkewitch (1953), Spriggs and Vasilos (1963), Knudsen (1959), Cutler (1957), and Choi *et al*. (1962) have investigated the room temperature dependence of strength on microstructures and/or processing in several refractory oxides. In these studies, the most significant factors influencing the strength of a crystalline material are density (or porosity) and grain size. A large grain boundary area associated with a small grain size is considered to prohibit dislocation movement at room temperature. For this reason, there is an increase in the strength of the material.

Plastic Deformation and Creep at High Temperatures

At elevated temperatures the role of dislocations and grain boundaries in crystalline material is considerably

complicated through the effect of the high temperature on the mobility of boundaries and dislocations. The dislocations already existing in the crystal become much more mobile. New slip systems become operative at high temperatures, resulting in increased flow and a consequent decrease in strength. This increased mobility of dislocations at high temperatures is responsible for the plasticity in refractory ceramic materials which are normally brittle at low temperatures (Wygant, 1951; Chang, 1959; Conrad, 1961, 1965; Wachtman and Maxwell, 1957; and Warshaw and Norton, 1962).

von Mises (1928) and Taylor (1938) pointed out that for a fine-grained polycrystalline solid to undergo plastic deformation, each crystallite must be completely capable of adjusting to the overall change in the shape of the neighboring grains. They further pointed out that to satisfy this condition, each individual crystalline grain must possess at least five independent slip systems. The deformation of crystals which do not have these systems must be accompanied by void formations in the grain boundaries. The identifying of ceramic materials by their various numbers of slip systems (Groves and Kelly, 1963; Copley and Pask, 1964) shows that none of the common ceramic materials have five independent slip systems at low temperatures except spinel and TiC; these refractory materials, however, do not have sufficient dislocation mobility at room temperature to permit

macroscopic plasticity. Stokes and Li (1963) have shown that polycrystalline sodium chloride deforms plastically above 150°C at which "wavy" or multiple slip is observed. The specimens failed by a necking process without developing grain boundary cracks or voids. Like magnesium oxide, sodium chloride has only two slip systems at low temperatures. However, at elevated temperatures three extra slip systems become operative, satisfying the von Mises-Taylor criterion for generalized plastic deformation of polycrystalline materials. Similarly, Pratt et al. (1964) showed that polycrystalline CaF_2 deforms plastically when five slip systems become operative at approximately 350°C.

Because the temperature range at which most ceramic materials satisfy the von Mises-Taylor conditions is so high, additional complications come into play. Thus the occurrence of plastic deformation in ceramic materials by simple dislocation movement is rarely observed.

When a polycrystalline mass undergoes a generalized volume-conservative deformation at elevated temperatures, it does so by deforming the crystalline grains and by sliding the grains past each other along grain boundaries. According to the most widely accepted theories, grains can deform either by some plastic mechanism involving dislocation motion or by a diffusion mechanism which was initially studied by Nabarro (1948) and later refined by Herring (1950).

The extent of plastic deformation by dislocation movement in a crystalline body depends primarily on two factors:

1) the total number of dislocations existing and newly generated in the grains, and 2) the mobility of the dislocations. During deformation, the dislocations sweep across the slip planes until they eventually pile up at various obstacles, e.g., sub-grain and grain boundaries (Mott, 1953). For further deformation to occur, these piled-up dislocations must climb over the obstacles by a diffusion process and continue to move. When the rate at which dislocations are pushed against the barrier is equal to the rate at which the dislocations overcome the barrier by climbing, a steady-state creep rate is established. The rate-controlling step in this process is the diffusion necessary to achieve dislocation climb. Utilizing this concept, Weertman (1955, 1957) has shown that the creep rate ($\dot{\epsilon}$) varies with the applied stress (σ) and the temperature (T) according to this relationship:

$$\dot{\epsilon} = A\frac{\sigma^n}{RT} \exp(-Q/RT) \qquad ---(3)$$

where Q is the activation energy for self-diffusion, R the gas constant, and A the proportionality constant. The exponent n is a constant varying from 3 to 4½. Chang (1960) found that the steady-state creep of single crystal aluminum oxide is controlled by the dislocation climb mechanism.

To date, creep behavior in most polycrystalline ceramic materials has been generally considered to be controlled by NaBarro-Herring type diffusion mechanisms previously mentioned. Herring proposed the following equation to relate the creep

rate ($\dot{\epsilon}$) to the temperature (T), the applied stress (σ), the grain size (d) of the polycrystalline body, and the diffusion coefficient (D):

$$\dot{\epsilon} = A \frac{\sigma D}{d^2 T} \qquad ---(4)$$

The linear relationship of $\dot{\epsilon}$ and σ in the equation indicates that the flow process is a viscous type controlled by vacancy diffusion in the lattice. Many research workers (Warshaw and Norton, 1962; Chang, 1959; and Folweiler, 1961) have shown that the activation energy determined from creep tests in polycrystalline aluminum oxide agrees well with that obtained from the sintering rate and internal friction methods, indicating that the creep process of this material is controlled by the Nabarro-Herring mechanism. The diffusion mechanism is controlled by the concentration of vacancies, their rate of migration through the lattice, and the state of stress. However, due to geometrical considerations, these mechanisms cannot operate extensively in a polycrystalline mass without some accompanying grain boundary motion. The dependence upon grain size is expressed as a power function proportional to d^{-2}.

Although attempts have been made to explain the creep mechanism in terms of the grain size of polycrystalline ceramics, e.g., Al_2O_3, all researchers do not agree on the nature of this mechanism. However, the work of Coble and Guerard (1963) seems to clear up the disparity concerning the creep mechanism of large-grained Al_2O_3. Accumulated experimental

evidence tends to demonstrate that creep in polycrystalline Al_2O_3 is a viscous flow regardless of grain size, although the recent results of Fryer and Roberts (1965) and Davis and Palmour (1964, 1965) suggest that plastic deformation on basal slip plane may be important in high purity polycrystalline alumina.

Creep by vacancy diffusion has also been observed in polycrystalline metals. According to Conrad (1961), Chen and Machlin (1957), and Gifkins (1956), even in ductile metals, void formation in grain boundaries which precedes the final weakening and failure of metal is an inevitable consequence of grain boundary shear. Intrater and Machlin (1959) observed that when bi-crystals of very pure (99.999%) copper are subjected to a shear force applied parallel to the grain boundary in an H_2 atmosphere, voids form with the number of voids increasing as the amount of grain boundary sliding increases. In vacuum, small cracks rather than voids form along grain boundaries. They concluded that voids and cracks nucleate due to the stress developed at the edge of a slip plane which is blocked by the grain boundary. Examination of the microstructure of extensively deformed pure aluminum revealed sliding of as well as migration of the grain boundaries (Chang and Grant, 1952, 1953).

EXPERIMENTAL PROCEDURE

Spinel Preparation

The mechanical properties of crystalline ceramic materials are greatly affected by the impurities they contain. Chang (1959) suggested that the proper type of impurities along grain boundaries can decrease the grain boundary "viscosity", resulting in a reduction of strength in polycrystalline materials. An increase in total purity by about 0.5% augmented the compressive strength of hot-pressed spinel by 10 fold from 2000 psi at 1600°C (Kriegel et al., 1964). The mechanical properties inherent in polycrystalline materials can thus be studied more effectively the purer the material. For this reason, and for the purpose of obtaining fine-sintered grain size, a chemical coprecipitation process was chosen for the synthesis of high purity spinel. A detailed procedure for coprecipitation and the subsequent calcination of high purity stoichiometric spinel powder is described by Kriegel et al. (1964). The process yields a soft, fluffy, friable powder with an ultimate particle size of approximately 40mμ as shown by electron microscopy in Figure 1.

Conversion of the powder to spinel was confirmed by X-ray diffraction. Spectrographic analysis showed the total impurity content to be about 0.06%, the chief ones being Si, Mn, Bi, and Sn. The mole ratio of Al_2O_3 to MgO was 1.065 as revealed by wet chemical analysis (Palmour et al.,

Figure 1. Electron micrograph of coprecipitated spinel powder

1963 b); in view of the small deviations and of the uncertainties involved in the analytical procedure, this spinel is considered to be essentially stoichiometric.

Initially, loosely bound soft lumps of calcined spinel were broken up by milling them in polyethylene bottles with Teflon balls to minimize contamination. However, both dry and wet (acetone) milling proved to be unsatisfactory in that hot-pressed samples of the milled powder had a black color indicative of a hydrocarbon pick-up from the plastic. As much as 5% weight loss was noted upon firing the dry-milled spinel at 1000°C for 50 hours in air. Even after this heat treatment, the black color was observed though its intensity was considerably diminished. Consequently the plastic jar mill was replaced with an alumina mill. Spinel was loaded into a 96% pure alumina-lined ball mill with an equal weight of alumina balls and tumbled for 30 minutes. At that time, visual examination of the charge revealed a thorough break-up. It is assumed that because they were soft, the aggregates were satisfactorily broken up within this milling time; it is further assumed that the ultimate size was not significantly altered by milling. X-ray diffraction indicated no alumina contamination. The powder was removed from the ball mill and stored in a plastic bag and in a desiccator to prevent water pick-up.

Sample Preparation

Equipment. The construction and components of the hot-pressing apparatus utilized in this work are described in detail elsewhere (Choi, 1962). In brief, the equipment consists of a graphite die, punches, a push rod, a susceptor cylinder for induction coupling, a fused silica envelope which contains the above parts, and finally the graphite lid. A motor generator unit was used as the power source for inductive heating. Carbon black was used for thermal insulation in various areas.

A manually operated hydraulic system provided the necessary pressure. The junction of platinum 10% Pt-Rh thermocouples was placed on the top of the die and the side of the upper punch for primary temperature measurements. In addition, an optical pyrometer was used to check these measurements by sighting on the bottom of the lower punch through the double-prism system. When temperature corrections were made for the prisms, there was 10°C difference at maximum at any given time between measurements by the two different methods.

Hot Pressing. Approximately 13 grams of ball-milled spinel powder were pre-pressed at room temperature in a hardened steel die under 20,000 psi utilizing a manually operated hydraulic press. Because of the fineness of the powder and because no binder or granulation was used to inhibit lamination, the pressure was increased successively

by 5000 psi increments and each time the entrapped air was released. After being ejected from the die, the pellet (1 inch in diameter by approximately 0.4 inches in height) was gently abraded against a nylon cloth to remove the iron particles which had abraded from the die wall and punch faces. A detailed description of the rate-controlled hot pressing procedure developed for high purity, fine-grained spinel has been previously described (Kriegel et al., 1964). In brief, the pellet was loaded into a low ash graphite die resting on three corks, and a preload of 300 psi was applied to the top punch through a graphite push rod. During the early stage of the heat-up process, the corks charred at 200° - 300°C into easily deformable charcoal which then pressed down in relation to the stationery bottom punch. This provided a double punch action, facilitating the development of uniform density in the pressed compact. As the temperature was further increased, spinel began to sinter, causing a downward movement of the top punch detectable by means of a sensitive dial gauge. Simultaneously the pressure was increased gradually to achieve rate-controlled hot pressing. This allowed the material to pressure-sinter in a manner which avoided undesirable pore entrapment. The final hot pressing conditions were 1550°C at 4500 psi for 2½ hours. Three compacts were not pressed under these conditions from which mechanical specimens were cut.

Determination of Microstructure

Density Determination. The bulk density of three hot-pressed compacts was measured by a suspended-weight method. The hot-pressed disc was cut into a 0.707 inch square which was then carefully washed in detergent by ultrasonic cleaning prior to density measurements. A more complete description of the density measurement technique as well as the equation utilized for calculation is presented elsewhere (Choi, 1962). The theoretical density attained was approximately 99.20% for all three compacts. The largest difference in density among the three samples was 0.02%. Thus, it was concluded that the density values were within the margins of experimental error.

Grain Size Measurements. Two specimens from each of the three hot-pressed compacts were mounted in cold-setting acrylic plastic and then polished successively with 14-, 6-, 1-, and ¼-μ diamond pastes on a vibratory polishing machine. After satisfactory polished surfaces were obtained, the specimens were removed from the mounts and etched with a concentrated reagent-grade sulfuric acid at 270°C. Constant acid concentration was maintained during etching by means of a reflux column; optimum etching conditions were thereby held constant for reliable reproducibility. The optimum etching time for revealing grain boundaries in hot-pressed spinel was 15-20 seconds.

Grain size counts were obtained from the photomicrographs of these etched surfaces. A detailed procedure for grain size determination from photographs is presented in a previous work (Choi, 1962). In the counting procedure, the number of grains intersecting each of six lines in a Latin square configuration (70 mm per line on the contact prints) was determined, and averaged, and the average number of microns per grain was ascertained. When measured this way the average grain size of hot-pressed spinel was about 0.54. There was no measurable difference in the average grain sizes between the two specimens from each hot-pressed compact. The typical microstructure of these hot-pressed compacts is shown in Figure 2.

Test Specimen Preparation

Cutting and Grinding. Utilizing a diamond saw, each of the three hot-pressed compacts was cut into 25 specimens measuring 0.130 inch by 0.130 inch by 0.40 inch. These specimens were mounted, ten at a time, on a steel carrier whose two faces had been ground previously for flatness and parallelism. Thermoplastic Acryloid was used for the adhesive agent. Then, all four longitudinal sides of each specimen were ground with an 80-grit diamond grinding wheel on a precision machine tool grinding table. Examination by micrometer showed that there were slight differences in the size of the specimens from lot to lot due to variations in the amount of material removed in clearing up the surfaces.

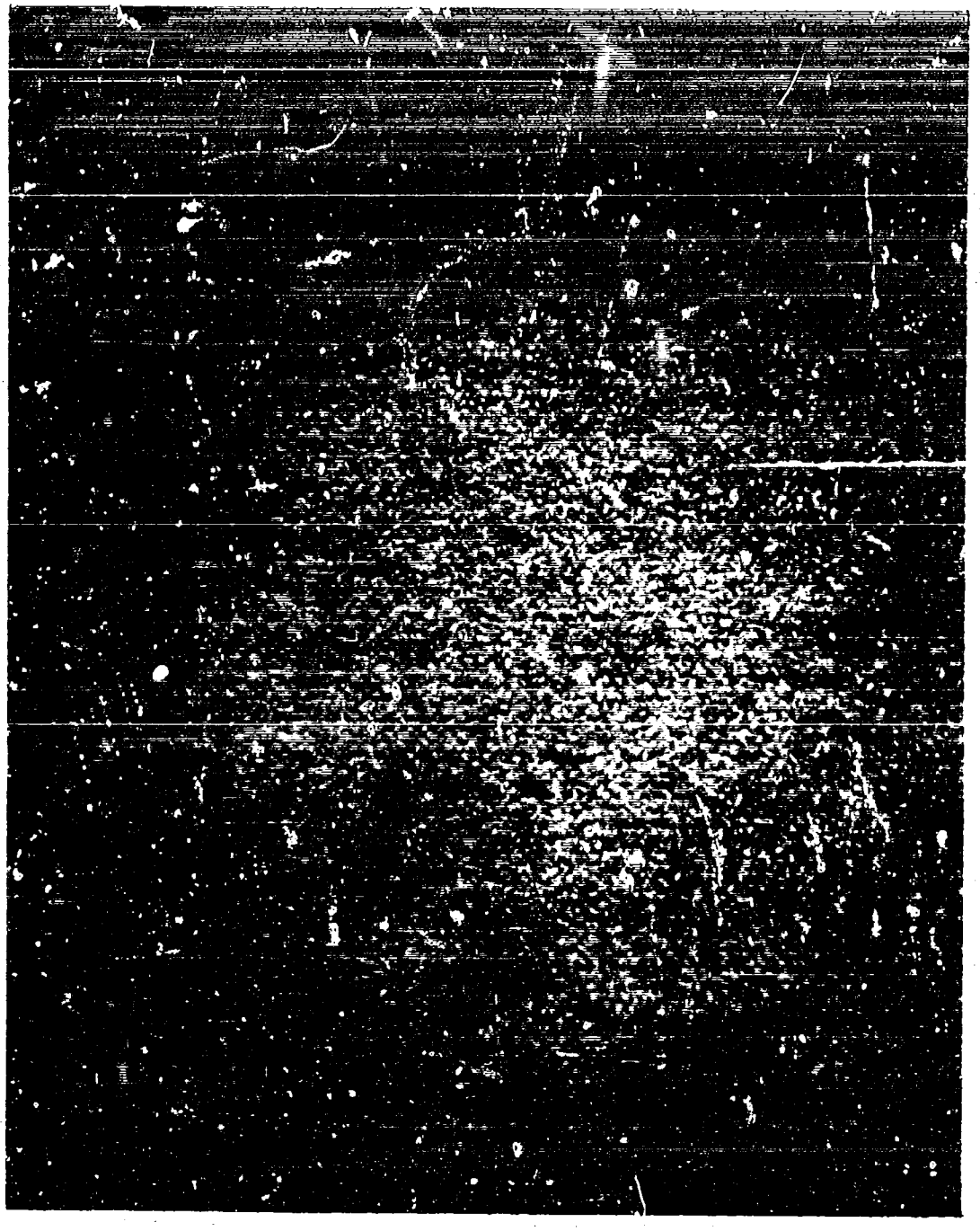

Figure 2. Microstructure of spinel hot pressed (1550°C, 4500 psi, 2½ hrs) by rate controlled method (average grain size 0.5μ). Chemically etched

However, satisfactory uniformity, parallelsim, and squareness of the ground surfaces of the specimens within each lot were achieved. Grinding of the two ends of the specimens was carried out in similar manner after they were heat treated (see next section). An extra precaution was taken in mounting the specimens on a special notched, reversible jig to make sure the ends would be ground perpendicular to the sides. A U-shaped groove with three flat sides held the specimens rigidly using Acryloid as thermoplastic adhesive. The final dimensions of the specimen after grinding were about 0.120 inch by 0.120 inch by 0.35 inch.

Heat Treatment for Grain Growth. Studies of the grain growth of oxides by heat treatment methods have been conducted by a number of research workers (Daniels et al., 1962; and Tier and Subbaro, 1963), including recent work by Spriggs et al. (1964) with fully dense hot-pressed magnesium oxide; samples of differing grain size were produced by heat treating dense fine-grained hot-pressed stock in air for various periods at different temperatures. In the present work, a similar procedure was employed. Hot-pressed spinel specimens were placed radially on one of their four ground sides in a small, high purity alumina crucible. Another Al_2O_3 crucible was used as a cover to prevent carbon from falling on the specimens during heat treating in the hot-pressing furnace. A third crucible (which rested upon a graphite disk on which an optical pyrometer was sighted)

supported the crucible containing the specimens so that they would not come in direct contact with graphite. Argon was allowed to flow into the furnace at the rate of 10 cubic feet per hour from the start to the end of heat treatment (including cooling). The temperature was increased at the rate of 25°C per minute until the desired level was reached. After soaking for the prescribed time, the power was cut off and the furnace cooled at its natural rate. After 12 trial firings, optimum temperature and time were determined for achieving the necessary grain growth for each grain size required for the experiment. The times at 1600°C for 1.7 μ and 10 μ grain sizes were 15 minutes and 60 minutes, respectively. At 1650°C the respective grain growth times for 60 μ and 200 μ were 45 minutes and 120 minutes. To approximately equalize the thermal history for all specimens, 0.5 μ specimens were heat treated at only 1350°C for 15 minutes without significant grain growth. The representative microstructures for these four grain sizes are presented in Figure 3.

Design of Experiment

The statistical design used in this experiment (Figure 4) has been described in a previous paper (Palmour et al., 1963 a). For this particular experiment, the three orthogonal axes (representing the three independent variables) were designated: 1) reciprocal absolute temperature, 2) natural logarithm of strain rate, and 3) natural logarithm of the grain size of the specimens. The experimental range for the variables

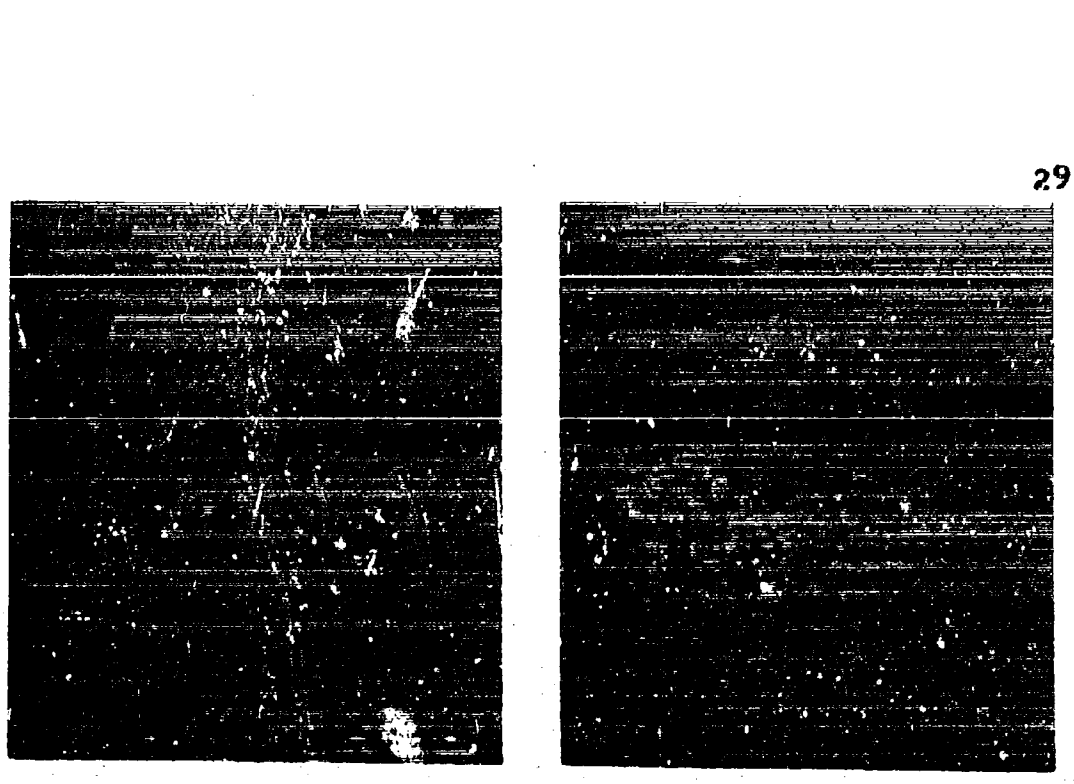

(a)

average grain size 1.7 μ

(b)

average grain size 10 μ

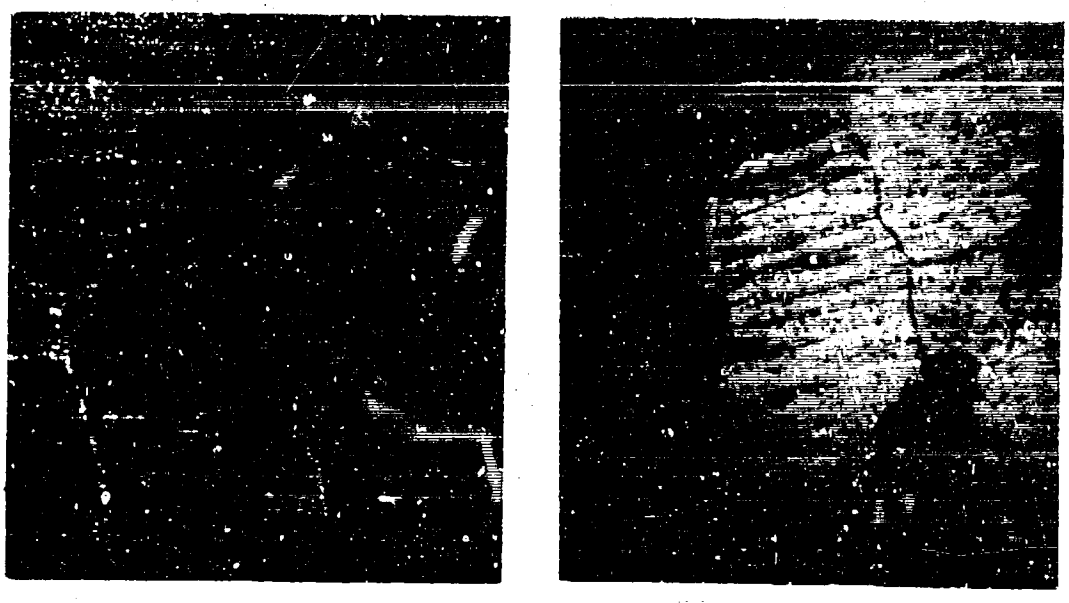

(c)

average grain size 60 μ

(d)

average grain size 200 μ

Figure 3. Microstructure of hot-pressed spinel upon subsequant heat treatment (described in text) to achieve grain growth. Chemically etched

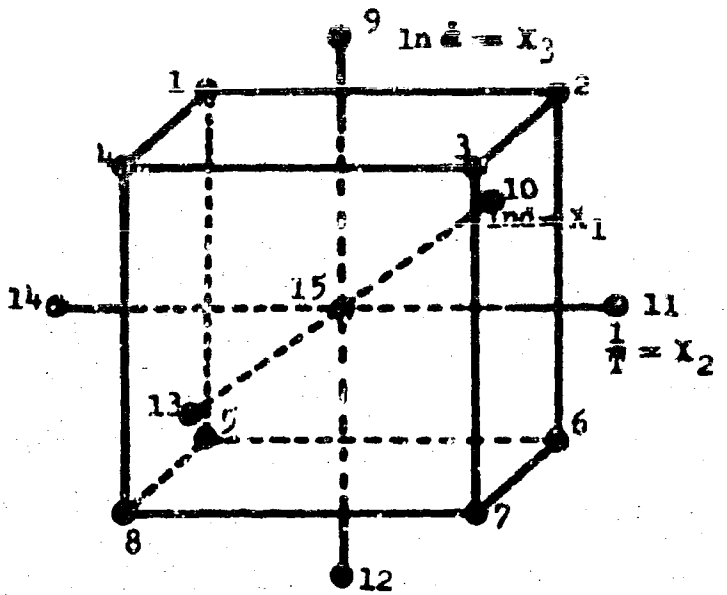

Experimental Point	Grain Size(d) in micron	Temperature(T) in ^{o}C	Strain Rate($\dot{\varepsilon}$) in $^{o}/o \cdot min^{-1}$
1	59.5	1691	1.97
2	59.5	1428	1.97
3	1.7	1428	1.97
4	1.7	1691	1.97
5	59.5	1691	0.127
6	59.5	1428	0.127
7	1.7	1428	0.127
8	1.7	1691	0.127
9	10.0	1550	5.000
10	200.0	1550	0.500
11	10.0	1353	0.500
12	10.0	1550	0.050
13	0.5	1550	0.500
14	10.0	1800	0.500
15	10.0	1550	0.500

Figure 4. Experimental design for determination of compressive flow stress as a function of grain size, temperature and strain rate

were selected on the basis of a preliminary study, as shown in Figure 4.

Three specimens, one from each of the three compacts, were tested at each of the fourteen outer experimental points and the results for each point were averaged. Six tests from each compact, a total of 18 were made at the center point.

Phenomenological Model for Plastic Deformation

The phenomenological creep equation by Zener and Hollomon (1944) has been modified for this experiment with addition of grain size d^{-m} to describe the deformation process in polycrystalline spinel. Thus the modified deformation equation is:

$$\dot{\epsilon} = A\sigma^{n} e^{-Q/RT} d^{-m} \qquad ---(5)$$

When this equation is rewritten, in logarithmic form, and when σ (the flow stress) is transposed to the left side of the equality, the new form of the equation becomes;

$$\ln\sigma = -\left(\frac{1}{n}\right) \ln A + \left(\frac{1}{n}\right) \ln \dot{\epsilon} + \left(\frac{Q}{nR}\right) \frac{1}{T} + \left(\frac{m}{n}\right) \ln d \qquad ---(6)$$

where n = exponent constant for flow stress

m = exponent constant for grain size

A = proportionality constant

$\dot{\epsilon}$ = strain rate

Q = apparent activation energy

R = gas constant

T = temperature

The statistical analysis method of Box and Hunter (1957) was employed in this experiment to establish a multiple quadratic regression describing the deformation process in hot-pressed spinel. The equation is composed of all the linear terms in Equation 6 as well as any statistically significant second order and interaction effects that may exist between the independent variables. The general form of the multiple quadratic regression is:

$$Y = b_0 + b_1 X_1 + b_2 X_1^2 + b_3 X_2 + b_4 X_2^2 + b_5 X_3 + b_6 X_3^2 + b_7 X_1 X_2 + b_8 X_1 X_3 + b_9 X_2 X_3 \quad \text{----(7)}$$

where $X_1 = f(\ln d)$

$X_2 = f\left(\frac{1}{T}\right)$

$X_3 = f(\ln \dot{\epsilon})$

$Y = f(\ln \sigma)$

d = average grain size, μ

T = temperature, $^\circ K$

$\dot{\epsilon}$ = strain rate, min^{-1}

σ = average flow stress, psi

An IBM-1410 computer was used to determine the response equation and the analyses of variance.

Compression Testing

Equipment. A floor model Instron physical testing machine[1]

[1]Instron physical testing machine, Model TTCLM, a product of Instron Engineering Corporation, Canton, Mass.

in conjunction with a Brew[1] furnace containing tantalum resistance heating elements and radiation shields were used for the compression testing of hot-pressed spinel specimens in vacuo at elevated temperatures. The Instron is capable of handling loads up to 10,000 pounds at strain rates of 2×10^{-5} in/min to 2 in/min. The 2500°C capability furnace is equipped with an automatic temperature control device for heating, soaking, and cooling. The hot zone is water cooled, with flow rates of water being kept constant during heat-up and during the testing period. The water pressure is controlled and maintained by a pressure regulator and a pump which draws the water from a reservoir tank. A small change in the water pressure (about 5 lbs) causes a fluctuation in temperature of approximately 1°C and a consequent change in the dimension of the load column resulting in a reduction or increase in the load on the specimen during testing. One degree centigrade drop in temperature induced approximately 1 lb of load decrease in the specimen.

The compressive load to the specimen was transmitted through two 3/4 diameter tungsten push rods, 6 inches in length, each attached to the crosshead and the load cell by means of adaptors. Since the test is very sensitive to the overall alignment of the load column with respect to the

---

[1]Brew Vacuum Furnace, Model 1064, a product of the Vacuum Equipment Division, Richard Brew Company, Inc., Concord, New Hampshire.

specimen, the two ends of each push rod were ground for flatness and parallelism, and were carefully aligned in the machine. In addition, a graphite ball-socket device was used to further increase the accuracy of the alignment. Previous tests (Palmour and Choi, 1963) showed that hot-pressed spinel specimens indented the tungsten push rods at temperatures above 1500°C. Thus, hot-pressed tantalum carbide pads, 7/16 inch in diameter by about 1/8 inch thick,[1] were employed as hard, strong anvils. Although tantalum carbide did not deform, it reacted slightly with spinel at temperatures above 1450°C. When thin tungsten sheet (0.002 inch thick) was inserted between the specimen and the TaC pads, the reaction was prevented. After the test, the tungsten shim was readily popped off the TaC surface with a razor blade. Due to the thinness of the shim, the small deformation which occurred immediately beneath the specimen was considered an insignificant factor in the overall measurement of strain. Figure 5 illustrates the several elements of the high temperature test assembly.

---

[1] In previous compressive tests, hot-pressed spinel pads were used as anvils, spreading the load to the tungsten. However, after only three usages the two compression sides had to be reground to remove the slight indentations beneath the sample. Tantalum carbide pads with approximately 92% theoretical density showed no structural deterioration even after usage of more than 40 heating-cooling cycles under loads up to 50,000 psi at temperatures as high as 1800°C. The pads were cut and ground from 7/16 inch diameter by 7/16 inch long slugs hot pressed by R. D. McBrayer and this writer in a graphite die in the Instron-Brew facility using the rate-controlled method.

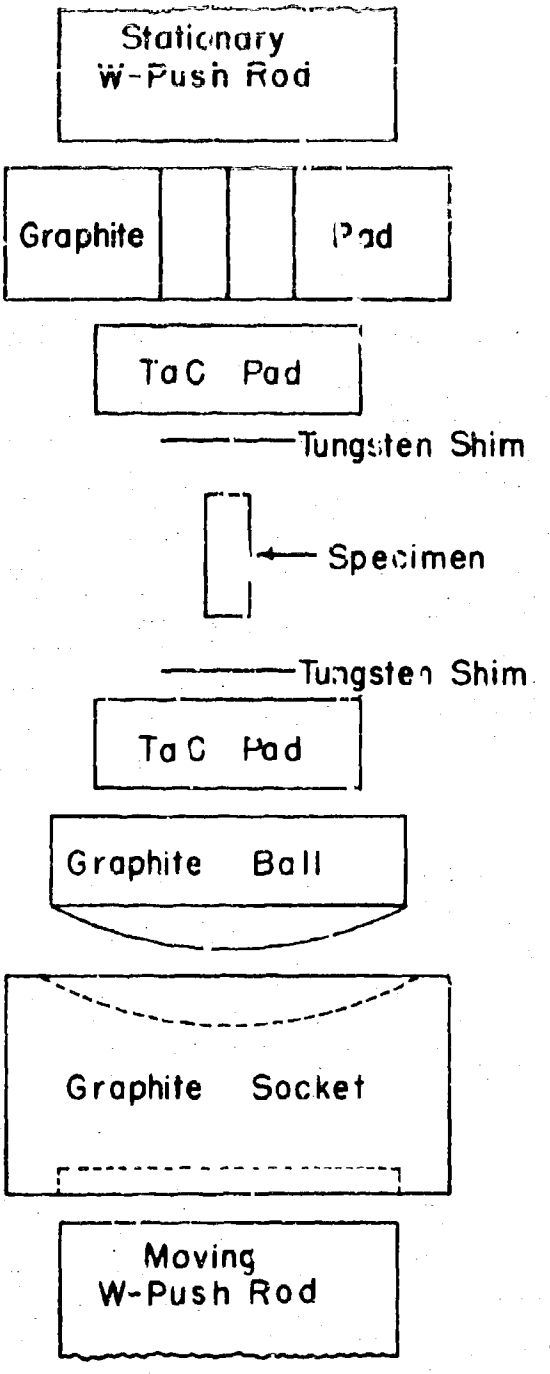

Figure 5. Schematic diagram of high temperature compressive loading assembly

Temperature measurements were made utilizing a W 3% Re-W 25% Re thermocouple connected to a recorder-controller, and above 1000°C, a two-color pyrometer with separate indicator-recorder capability. The thermocouple is located about 2½ inches below and about ¼ inch laterally away from the specimen. The temperature measurements by these methods were periodically checked with a disappearing filament optical pyrometer. Both pyrometers were focused on a V-notch on a graphite pad which was in direct contact with the upper tungsten push rod. The temperature measured by focusing the pyrometer on the specimen was somewhat higher than that measured on the graphite pad due to the specimen's increased reflectivity. The graphite with its V-notch approximately simulates a black-body condition.

Testing Procedure. The test specimens were carefully cleaned with ethyl alcohol and cotton swab; the tungsten shims as well as the TaC pads were cleaned in the same manner. After dimensions were measured by a micrometer, the specimen was placed on the center of the shim (about 0.25 inch x 0.25 inch) which, in turn, rested on the center of the TaC pad. The same arrangements were made for the upper end of the specimen. Then, the entire assembly was held as a unit by the spring action of a special molybdenum jig. The device keeps the various individual parts in place while the assembly is placed on the center of the graphite ball-socket resting on the bottom push rod. After setting the upper graphite member

and centering it on the top of the assembly, the socket was adjusted so that the upper tungsten push rod was in uniform contact with the graphite pad. Having done so, the crosshead was slowly brought up until 10 lbs of load were registered on the recorder. The molybdenum jig then was removed from the loaded assembly without loss of specimen geometry. The crosshead was then lowered to release the load, and the symmetry, flatness, and evenness of contact between the graphite pad and the upper push rod was checked and readjusted. Finally, the specimen was reloaded and the crosshead was cycled between 10 and 14 lbs of load while the cooling water was turned on and during pump down and heat-up. Automatic retraction of the crosshead (proportional to thermal expansion in the furnace components) keeps the load cycling at an approximately constant level, 10 lbs during the entire pretest cycle.

The temperature was increased automatically at 50°C/min until the prescribed temperature was reached. The furnace soaked at constant power input until its components came to thermal equilibrium at the test temperature. After the crosshead ceased to move downward, as indicated by the constant gauge length, ten minutes were allowed to permit temperature stabilization. At this time, the partial pressure, about 2×10^{-5} torr, was checked, the cycling was stopped, the load was brought to zero and the recorder was rebalanced. Care was exercised to see that the load on the specimen was

in fact at zero load and that the push rod was still in contact with the specimen. Now, the actual testing was initiated at a preset-crosshead speed. All the tests were carried out under constant strain-rate conditions according to the experimental design. During the entire period of actual testing the furnace partial vacuum pressure remained approximately constant. However, from run to run the pressure varied from 1 x 10^{-5} to 2 x 10^{-5} torr. After a test was completed, the furnace was "quench" cooled by cutting the power. Simultaneously, the crosshead was lowered to avoid further deformation of the specimen. Three specimens. one from each compact, were tested at experimental points 1-14 (see Table 1 for exception). For experimental point 15 (the mid point) as called for in the design, 18 specimens were tested (six from each compact).

RESULTS

The results obtained in this experiment are systematically revealed in Tables 1 and 2, and Figures 6 through 16. This presentation aims primarily at clarifying and highlighting the results which are therein displayed.

Compression Testing

The compressive strength of each hot-pressed spinel specimen is given in Table 1. Stress-strain diagrams are presented in Figures 6, 10, 12 and 13. These curves illustrate typical tests at each of the fifteen experimental points. In obtaining the measurements of compressive stress, no corrections were made for the increase in the load area of the specimens due to deformation, nor for the small increase in area due to thermal expansion of the sample itself. It is proper to describe these as engineering stress-strain curves.

For all specimens, after a period of constant stress, a decrease in stress occurred at which point the test was concluded immediately by unloading. This constant stress is designated in this report as steady-state flow stress. During the early stage of unloading, brittle fracture occurred only in coarse grained specimens which were tested at high strain rates at low temperatures. Basically all the curves are similar in character, differing principally in the level of initial flow stress (stress at the proportional

limit) in the slope of increasing stress with increasing strain above the proportional limit, and in the amount of steady-state flow strain. The results of these tests are presented in the following sections according to the strain rates under which the specimens were tested.

Table 1. Dependence of steady-state flow stress of hot-pressed spinel on temperature, strain rate, and grain size

Experimental Point	Temperature (°C)	Average Grain Size (μ)	Strain Rate (%/min)	Flow Stress (psi) Specimen (1)	(2)	(3)	Average Flow Stress (psi)
1	1691	59.5	1.97	17,500	15,450	18,650	17,200
2	1428	59.5	1.97	24,500	31,200		27,900
3	1428	1.67	1.97	48,500	37,600	53,500	46,500
4	1691	1.67	1.97	16,400	10,200	16,200	14,300
5	1691	59.5	0.127	7,150	6,720		6,940
6	1428	59.5	0.127	12,900	15,400		14,200
7	1428	1.67	0.127	35,600	28,250	28,750	30,900
8	1691	1.67	0.127	3,220	3,300		3,260
9	1550	10.0	5.000	33,500	38,000	43,600	38,400
10	1550	200.0	0.500	14,360	14,200		14,300

(continued next page)

Experimental Point	Temperature (°C)	Average Grain Size (μ)	Strain Rate (%/min)	Flow Stress (psi) Specimen (1)	(2)	(3)	Average Flow Stress (psi)
11	1353	10.0	0.500	60,000	44,300		52,200
12	1550	10.0	0.050	6,690	5,032	6,550	6,220
13	1550	0.5	0.500	21,200	15,100	16,400	17,600
14	1800	10.0	0.500	2,150	1,860	2,500	2,170
15	1550	10.0	0.500	21,500	23,700	20,600	20,300
				(4) 15,400	(5) 19,500	(6) 18,700	
				(7) 17,600	(8) 24,200	(9) 17,100	
				(10) 16,900	(11) 17,700	(12) 23,300	
				(13) 26,000	(14) 22,700	(15) 12,200	
				(16) 25,200	(17) 25,800	(18) 16,000	

Low Strain Rate (0.127%/min). Figure 6 shows stress-strain plots for specimens having small (1.67μ) and large (60μ) grain size; typical test data obtained at both 1428°C and 1691°C for each grain size are illustrated. Both sets of specimens were tested under the same low strain rate and none failed by fracture. There are several interesting features in this figure. At 1691°C, the initial flow stress of the small-grained specimen (curve D) was much lower than that of the large-grained specimen (curve C), whereas the results were reversed when testing was carried out at the lower temperature of 1428°C. The other point of interest is that regardless of the test temperature, the steady-state flow strains of the smaller-grained specimens were greater than those of the larger-grained specimens. At 1428°C there is no difference in the apparent Young's modulus of elasticity attributable to the two grain sizes. However, the nominally linear initial portion of the stress-strain diagram has a much lower slope for the small-grained specimen at 1691°C than for the larger-grained specimen. Figure 7a shows preferential crack formation near the ends of a 1.67μ specimen deformed at 1691°C (curve D, Figure 6). Note that most of the cracking is confined to the regions where end constraint accounts for a complex state of stress, and that these shear cracks spanning many grains were neither continuous nor catastrophic. Conversely, predominantly intergranular cracks are observed in the 60μ specimen tested at 1428°C (Figure 7b),

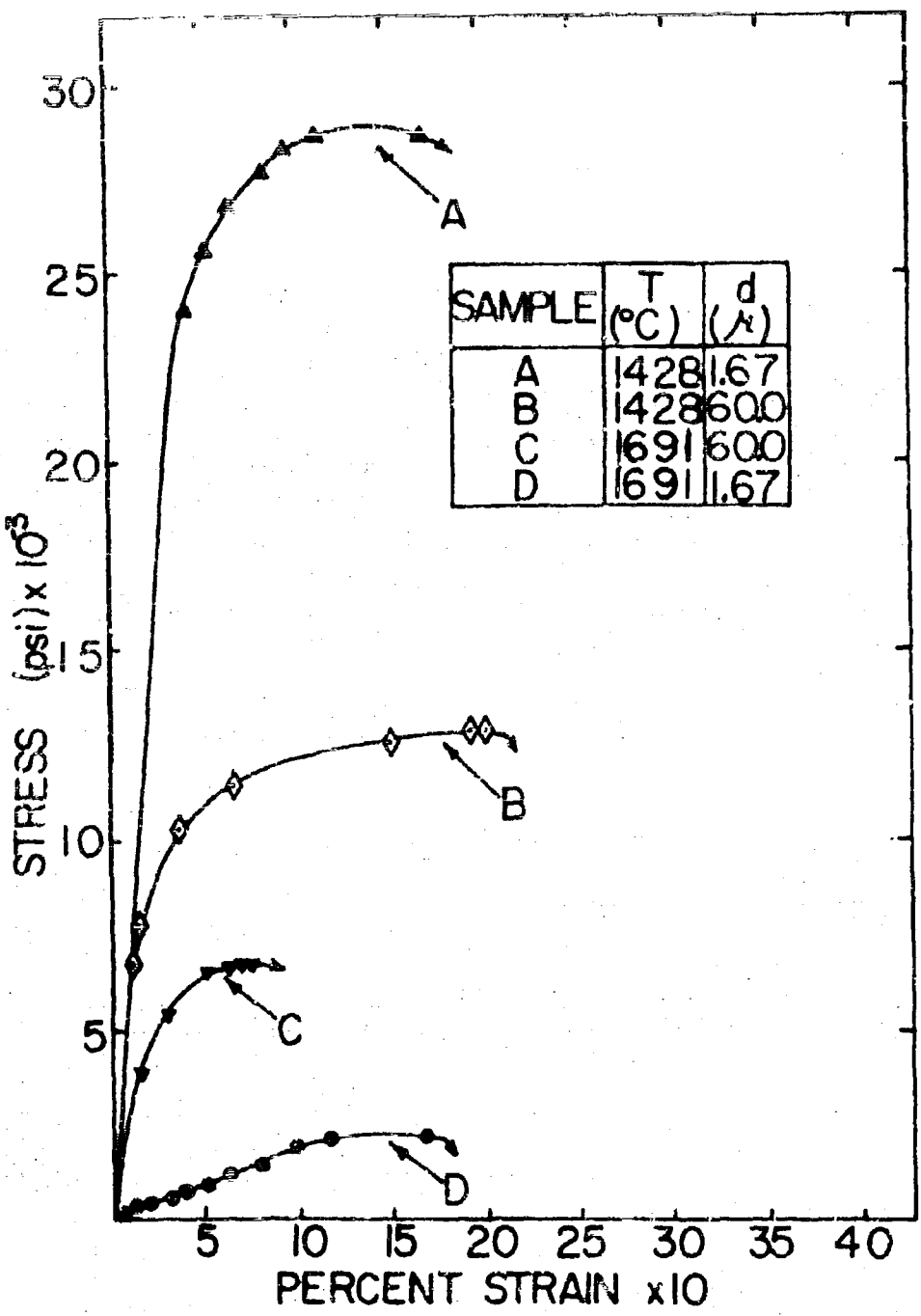

Figure 6. Typical stress-strain diagrams for hot-pressed spinel specimens deformed in compression at a strain rate of 0.12%/min

(a)
1.7μ, 1691°C, 0.127%/min

(b)
60.0 μ, 1428°C, 0.127%/min

(c)
1.7μ, 1428°C, 0.127%/min
(before inking)

(d)
1.7μ, 1428°C, 0.127%/min
(after inking)

Figure 7. Surface texture of deformed spinel specimens. Illumination normal to viewing axis, from left and right. Load axis vertical, X 12

and they are much more uniformly destributed throughout the test specimen. Figure 7c was taken from the 1.67μ specimen tested at 1428°C. An attempt was made to identify the fine lines in this specimen which intersect at an angle of approximately 120° by applying ink with a brush to the surface. After the ink dried, the surface was wiped off with a wet cloth. This surface was then re-photographed (Figure 7d) under lighting and exposure conditions identical with that for Figure 7c. The comparison of these photographs clearly shows that the original fine lines became darker when dyed by the ink, thus indicating that they are crack lines. From the photograph it is also evident that more cracks or voids developed close to the constrained ends than did near the center portion. A closer look (Figure 8) revealed additional evidence that these fine lines are in fact cracks formed principally along the maximum shear planes. Figure 8 was obtained from a chrome-shadowed replica of the thermally etched surface which had been pre-ground with an 80-grit diamond abrasive wheel before testing. There is some evidence of a "worked" texture, which in this case is considered to be an artifact resulting from grinding. The crack paths appear to be partly intergranular, partly transgranular. The replicas from the surfaces of the small-grained (1.67μ) specimens showed that after testing, at both temperatures the grains had grown to approximately 5 times their original size. This may be partly due to a strain annealing effect

Figure 8. Microstructure of hot-pressed spinel specimen (1.7 μ) deformed at 0.127%/min at 1428°C. Chrome-shadowed replication photomicrograph

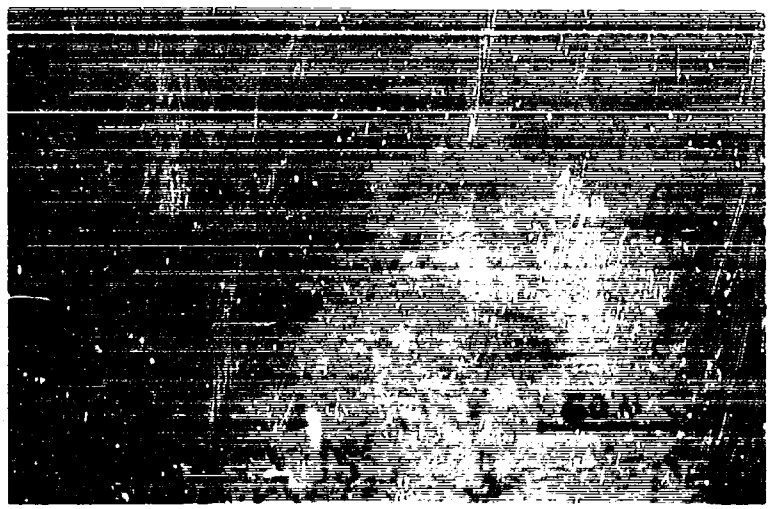

(a)

wavy and straight slip markings

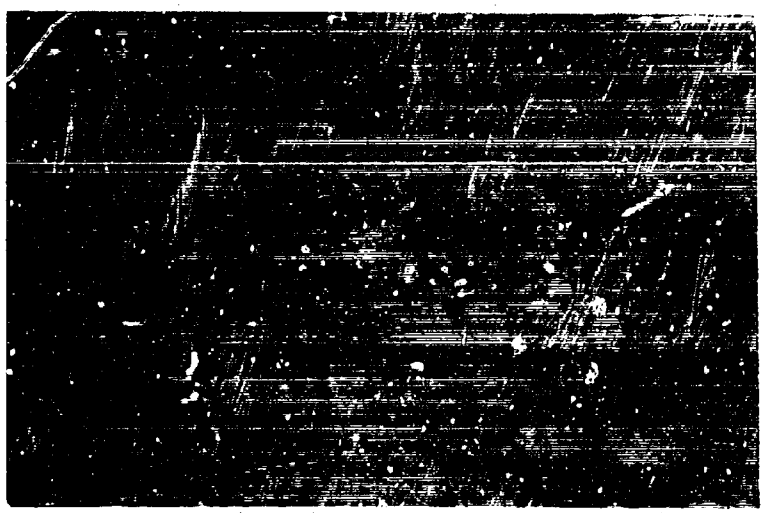

(b)

recrystallization

Figure 9. Microstructure of hot-pressed spinel specimen (60μ) deformed at 0.127%/min at 1691°C. The specimen surface was mechanically and then chemically polished prior to test

in which excessive strain energy caused by plastic deformation is reduced, and also partly involving some vacancy and ionic diffusion process of the Nabarro-Herring type. A careful examination of all specimens after testing showed that these fine interpenetrating cracks were observed only in specimens tested at this one experimental combination (1.67μ, 1428°C, 0.12%/min).

Prior to testing at 1691°C the 60μ specimen was polished with diamond pastes, 14μ, 6μ, and 1μ successively, and the polished cold-worked layer was chemically removed by heating the specimen at 270°C in concentrated sulfuric acid for 30 seconds. Even though much surface gloss was lost by thermal etching during testing in vacuo, the specimen did retain a sufficient amount of surface reflectively after testing to permit photomicrography. Photomicrographs of the surface illuminated with reflected light are shown in Figure 9. Here the first photograph (Figure 9a) contains a large number of straight and wavy slip markings which cover two or more grains. It also shows intergranular cracks located immediately adjacent to these markings, and the etch pits attributable to dislocations are revealed in favorably oriented grains.

The outstanding feature in Figure 9b is the large number of new small grains within the pre-existing grains. These new grains were likely formed by recrystallization - a process involving polygonization which is common in heavily deformed metals at elevated temperatures.

Medium Strain Rate (0.5%/min). There are, in all, five stress-strain curves in Figure 10. These curves represent tests of 0.5%/min on five specimens, three of which measured 10 μ in grain size and were tested at 1353°C, 1550°C, and 1800°C, respectively. For the other two specimens, one 0.5μ and one 200μ, both were tested at 1550°C. The general shape of the two curves for the 0.5μ specimen and the specimen tested at 1800°C is quite different from the shape of the other three curves. Their initial flow stress and apparent Young's moduli are much lower, while their total plastic deformation is considerably higher than the rest. For the 0.5μ specimen (curve E, Figure 10), the steady-state flow condition is achieved after approximately 6% of permanent deformation. Only occasional small islands of cracks (or pores) were revealed by the inking test on the 10μ specimen tested at 1800°C. After a very limited indication of steady state flow, the specimen tested at 1350°C (curve A, Figure 10) failed audibly, breaking into several small pieces.

The 200μ specimen (curve C, Figure 10) was specially prepared prior to testing by mechanical polishing and chemical treatment in the manner described earlier for microscopic observation. The failure mode for this specimen was entirely different from that of the others tested. It broke into small equiaxed fragments which had approximately a uniform size, about 1 mm in diameter. However, the pieces close to the compressive ends of the specimen were large

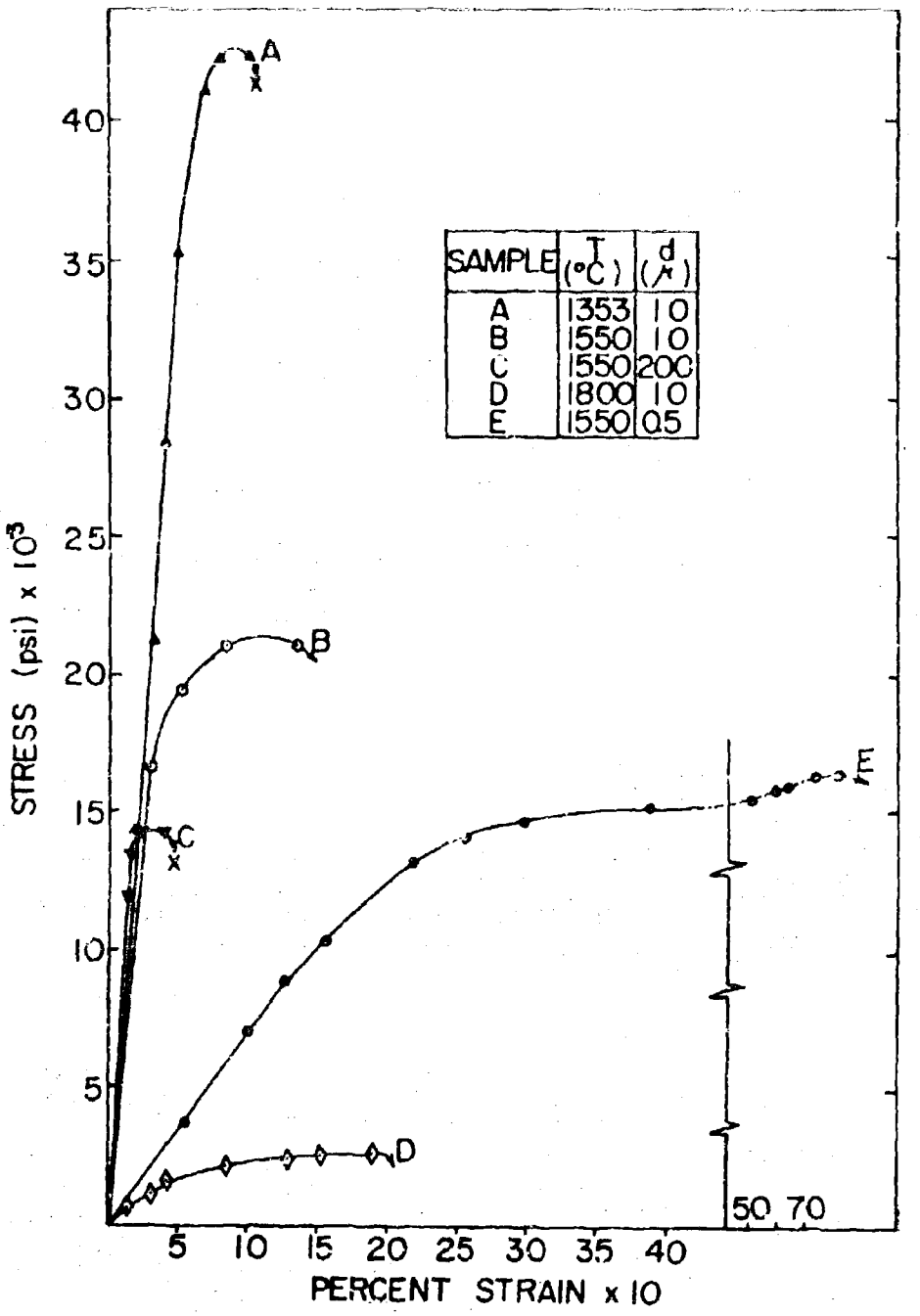

Figure 10. Typical stress-strain diagrams of hot-pressed spinel deformed in compression at a strain rate of 0.5%/min

enough to use for microscopic examination as is shown in Figure 11. Here the first two photographs (a and b) show a large number of wavy slip lines within the grains. The development of intergranular cracks at Y-junctions (three-grain intersections) is also clearly indicated.

The third photograph (c) displays a transgranular crack formed near such a Y-junction. In addition to crack formation, grain boundary sliding may also have occurred in some regions of this specimen as is shown by the apparent displacement of the remanent scratch lines in Figure 11d. The scratch lines in grain A are slightly out of focus and hence appear broader than they actually are; it appears that grain B has displaced to the right and into the background.

High Strain Rate (1.97%/min). The grain size and testing conditions for the specimens represented in the stress-strain curves of Figure 12 are identical with those in Figure 6. The only difference in the strain rate which in Figure 12 is 1.97%/min, or over an order of magnitude larger than the rate for the specimens in Figure 6, 0.127%/min. The steady-state flow stress of all specimens tested at the strain rate of 0.127%/min is lower than that of their corresponding specimens tested at 1.97%.min. With one exception (1.67μ at 1691°C) the total plastic strain of the specimens tested at 0.127%/min is larger than the strain of those tested at 1.97%/min. Three of the four specimens tested at the higher rate (Figure 12) broke while unloading whereas none tested at the lower rate did (Figure 6).

(a)

wavy slip and
intergranular crack

(b)

wavy slip and
intergranular crack

(c)

transgranular crack
at Y-junction

(d)

apparent grain
boundary sliding

Figure 11. Microstructure of hot-pressed spinel specimen (200 μ) deformed at 0.5%/min at 1550°C. The specimen surface was mechanically and then chemically polished prior to test

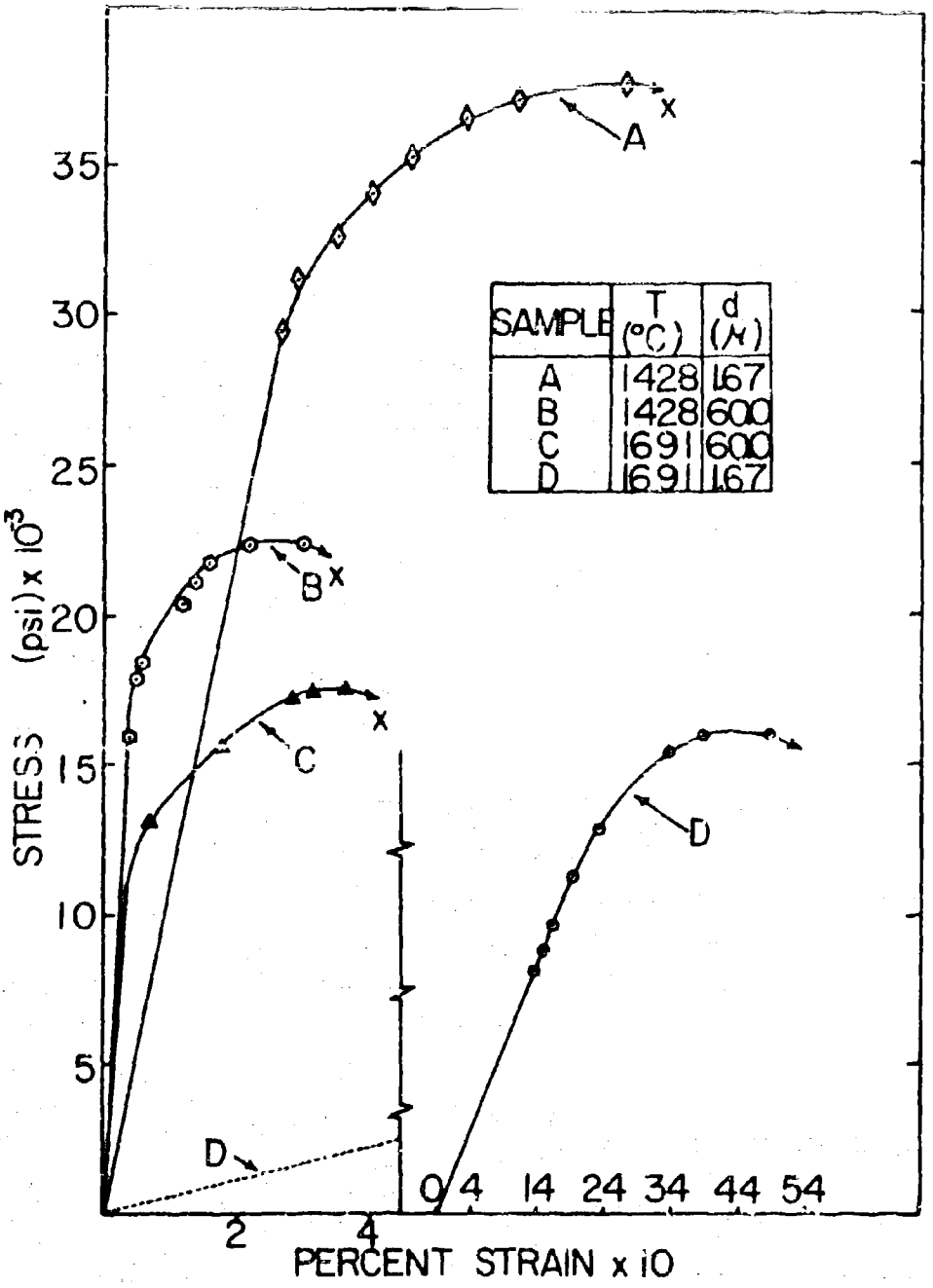

Figure 12, Typical stress-strain diagrams of hot-pressed spinel deformed in compression at a strain rate of 1.97%/min

Highest and Lowest Strain Rate (5%/min, 0.05%/min). The two stress-strain curves shown in Figure 13 represent the two extreme strain rates employed in the compression testing of spinel specimens; the grain size and test temperature was identical for each. It is apparent that very little plastic deformation occurred in the specimen before failure by audible fracture at 5%/min strain rate. The specimen separated approximately along a maximum shear plane into two pieces. At 0.05%/min the specimen began to flow at a low stress level. The inking test was applied to the 0.05%/min specimen. The two constrained ends dyed dark, indicating the presence of ductile cracks in the specimen.

Kinetics of the Flow Process

Data reduction and analysis by an IBM - 1410 computer resulted in the following deformation equation, relating flow stress (σ) - the dependent variable in this experiment - to absolute temperature (T), strain rate ($\dot{\epsilon}$), and grain size (d) - the independent variables in this experiment:

$$\ln \sigma = -40.1089 + 2.1382\ (\ln d)^{*} + 157609.6468\ (\tfrac{1}{T})^{*} - 120374667.9(\tfrac{1}{T})^{2\,**} + 2.0003\ (\ln\ )^{**} - 3950.5969(\tfrac{1}{T})\ (\ln d)^{*} - 3010.6217(\tfrac{1}{T})\ (\ln \dot{\epsilon})^{***} \quad ---(8)$$

---

*Coefficient significant at 99% confidence limit

**Coefficient significant at 95% confidence limit

***Coefficient significant at 90% confidence limit

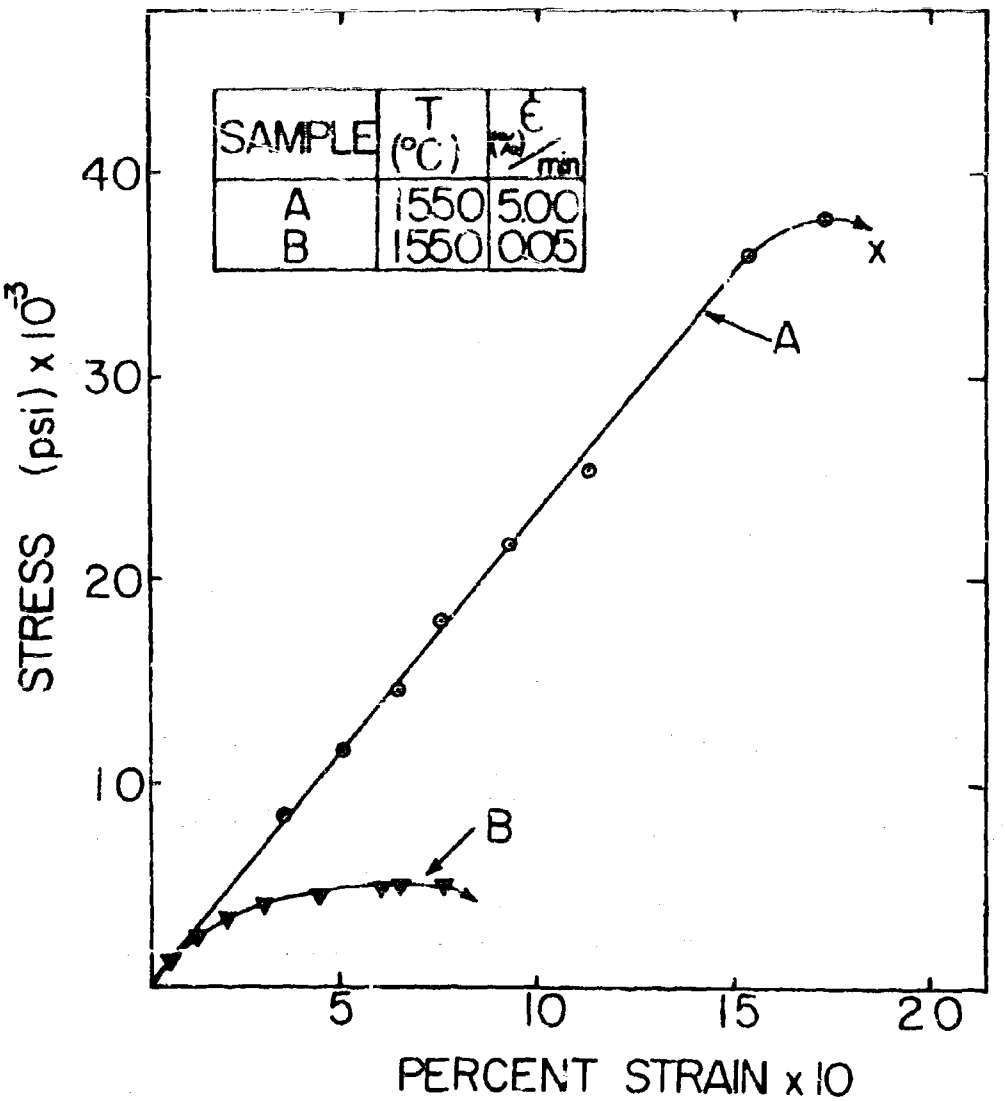

Figure 13. Typical stress-strain diagrams of hot-pressed spinel (10 μ) deformed at 1550°C in compression at two different strain rates

The data was [illegible] at least 90% predictability. Thus, only those terms which are significant at F = 3 (90%) level or at higher levels are included in this equation. The maximum difference between the steady-state flow stress obtained by computation from this equation and the average of actual measured values for any given experimental point is slightly over 5%. Thus Equation 8 is highly reliable in predicting the steady-state flow stress (σ) in terms of the independent variables. Taking the anti-logarithm of the equality, Equation 8 becomes:

$$\sigma = \left[e^{-40.1089}\right] \cdot \left[d^{2.1382}\right] \cdot \left[e^{157609.6468\left(\frac{1}{T}\right)}\right] \cdot \left[e^{-120374667.9\left(\frac{1}{T}\right)^2}\right] \cdot \left[\dot{\epsilon}^{2.0003}\right] \cdot \left[d^{-3950.5969\left(\frac{1}{T}\right)}\right] \cdot \left[\dot{\epsilon}^{-3010.6217\left(\frac{1}{T}\right)}\right] \qquad ---(9)$$

When the same variable terms and exponent terms are combined, Equation 9 yields,

$$\sigma = \left[e^{-40.1089}\right] \cdot \left[d^{2.1382\left(1-\frac{1847.63}{T}\right)}\right] \cdot \left[\dot{\epsilon}^{2.0003\left(1-\frac{1505.09}{T}\right)}\right] \cdot \left[e^{157609.65(?-\frac{763.75}{T})}\right] \qquad ---(10)$$

If the last term in the above equation is made to contain R, the gas constant, then Equation 10 can be rewritten into Equation 11 in a form that includes the apparent thermal activation energy related to the deformation of hot-pressed spinel:

$$\sigma = \left[e^{-40.1089}\right] \cdot \left[d^{2.1382\left(1-\frac{1847.63}{T}\right)}\right] \cdot \left[\dot{\epsilon}^{2.0003\left(1-\frac{1505.09}{T}\right)}\right] \cdot \left[e^{\frac{313170.37}{RT}\left(1-\frac{763.75}{T}\right)}\right] \qquad ---(11)$$

The general form of this equation is:

$$\sigma = K\left[d^{m(1-\frac{A}{T})}\right]\cdot\left[\dot{\epsilon}^{\frac{1}{n}(1-\frac{B}{T})}\right]\cdot\left[e^{\frac{Q}{RT}(1-\frac{C}{T})}\right] \qquad ---(12)$$

where K is 3.844×10^{-16} and the exponents expressing grain size, strain rate and thermal activation contributions are themselves temperature dependent (see Table 2). This equation is somewhat analogous to the creep rate equation proposed by Zener and Hollomon (1944):

$$\dot{\epsilon} = A\sigma^{n} e^{-Q/RT} \qquad ---(13)$$

The differences between Equation 12 and 13 are:

1) the dependent variable in this research is σ and not $\dot{\epsilon}$,
2) Equation 12 includes a power dependence upon the increase in grain size d, and
3) Equation 12 includes the interaction of grain size and temperature and strain rate and temperature, as well as the quadratic dependence upon temperature of the apparent activation energy.

Table 2 lists the calculated m, n and Q values obtained by substituting various temperatures in Equation 11. Because the dependent variable in this research is the steady-state flow stress rather than the strain rate the magnitude of Q value in this table cannot be compared directly with the activation energies that may be obtained from static stress creep tests where strain rate is the dependent variable.

Table 2. Temperature dependence of grain size-stress coefficient (m), strain rate-stress coefficient (n), and apparent activation energy (Q)

T, °C	m	n	Q(Kcal/mol)
1353	-0.291	6.725	166.07
1428	-0.184	4.340	172.58
1550	-0.029	2.860	181.97
1691	0.127	2.039	191.39
1800	0.233	1.825	197.79

Plot of $\ln\sigma$ versus $\ln\dot{\varepsilon}$, Figure 14, shows the increase in the slope, $\frac{1}{n}$, hence decrease in n values, with increasing temperature. This figure was constructed by substituting the actual temperatures and grain sizes as well as the strain rates employed in the experiment to the deformation equation, thus obtaining the computed stress values. For comparison between the actual data value and the predicted values, two of the actual data obtained in the experiment are plotted at 1550°C. As can be seen they agree very nicely. These results give values of n ranging from about 2 at 1800°C to about 7 at 1350°C. The work by McBrayer (1965) on single crystal spinel and the transverse testing of hot-pressed spinel by Palmour (1965) have shown n values ranging from 2 to 4 for single crystals, and 2 to about 5, averaging 2.7 for polycrystalline spinel in bending.

Figure 14 also illustrates the dependence of the flow stress on the grain size. The variation of the flow stress

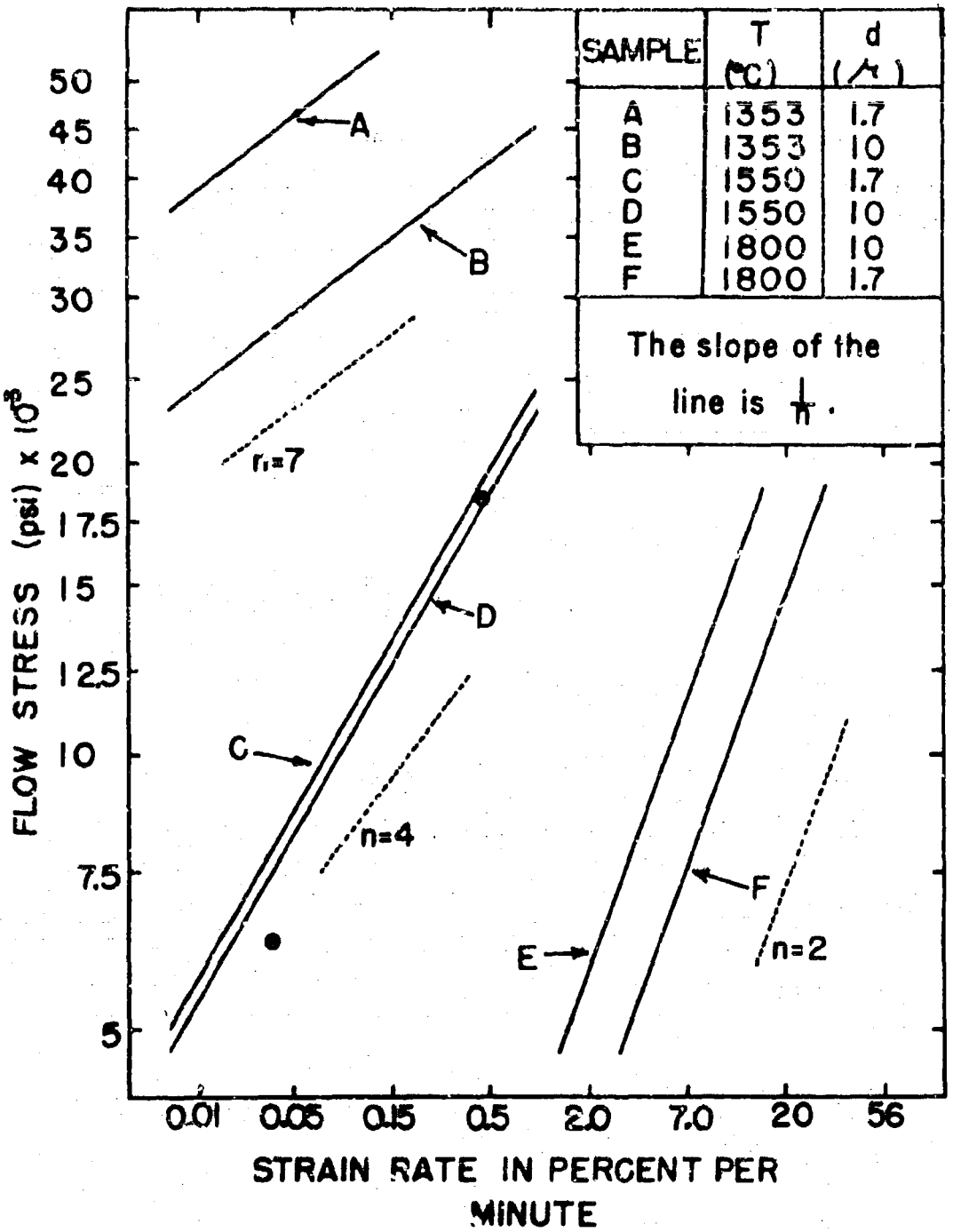

Figure 14. Logarithmic plot of stress as a function of strain rate computed for hot-pressed spinel deformed in compression

with grain size is comparatively large when tested under constant strain-rate at low and high temperatures (1353°C and 1800°C), and furthermore, the effect reverses at low and high temperatures. However, at 1550°C, there is very little flow stress change for 1.7μ and 10μ grain sizes when tested under the same strain rate. When m equals zero, the effect of variation of grain size on flow stress will vanish; the m values in Table 2 indicate that this temperature will lie somewhere above 1550°C.

The plot of m versus temperature in Figure 15 shows that it is zero at approximately 1575°C and illustrates parabolic temperature dependence. Figure 16 shows the plot of $\ln \dot{\epsilon}$ versus $\frac{1}{T}$, and contains the results of this study, along with data obtained in compression for alumina rich single crystal spinel, $MgO \cdot 3Al_2O_3$ (McBrayer, 1965) and in bending in polycrystalline spinel (Palmour, 1965). Above 1550°C, there is good agreement between the apparent activation energies obtained by the two different test methods, approximately 100-250 Kcal/mol for compression and 214 Kcal/mol for transverse. The apparent activation energies of single crystal (approximately 130 Kcal/mol) and polycrystals also agree well.

The curves for polycrystalline spinel clearly indicate the quadratic dependence of thermal activation in compressive deformation. The curves diverge in both directions from approximately their mid-points (1550°C, 0.001%/min), largely due to the grain size- and strain rate-temperature

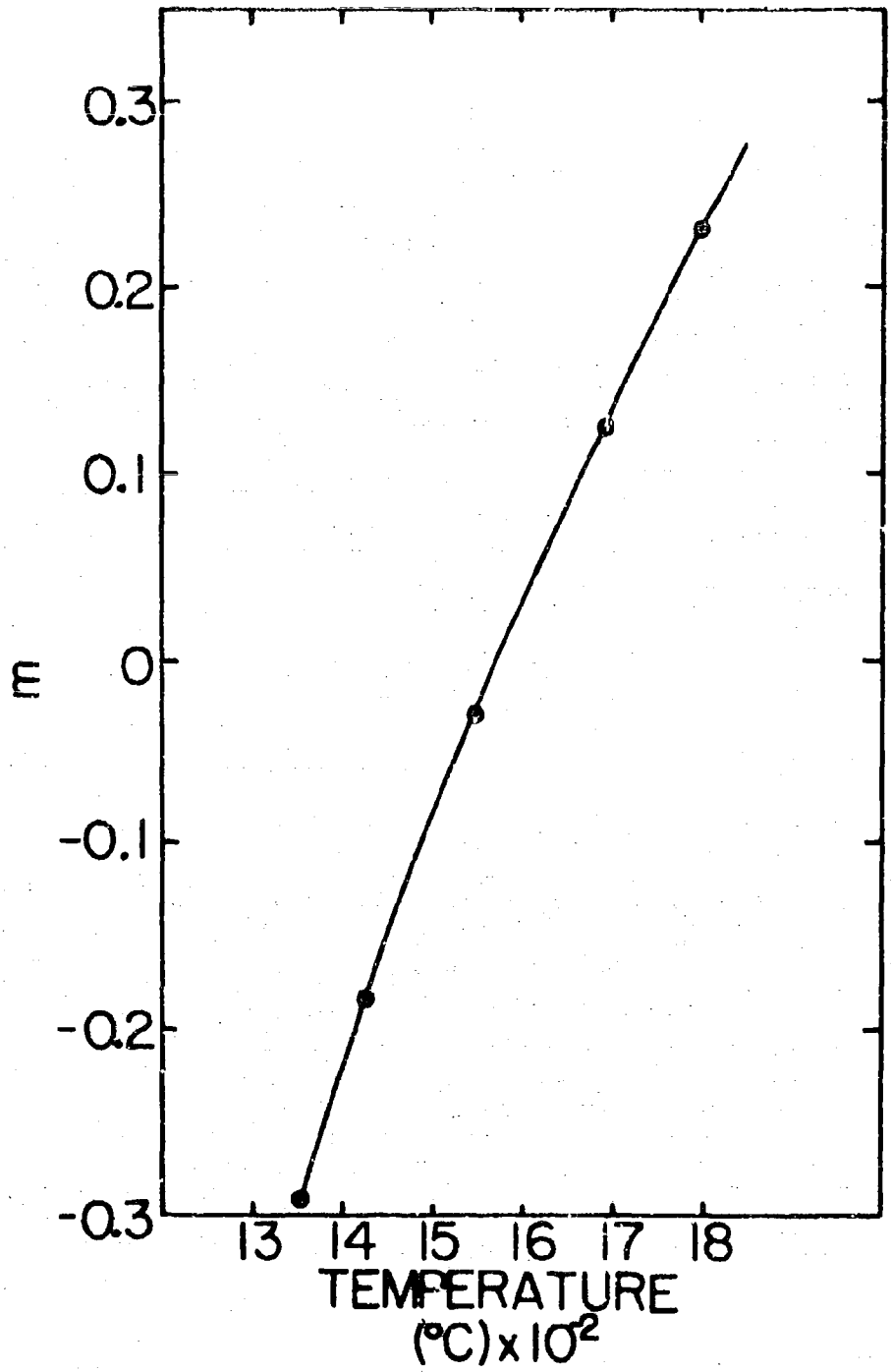

Figure 15. Variation of m, the grain size exponent, computed as a function of temperature

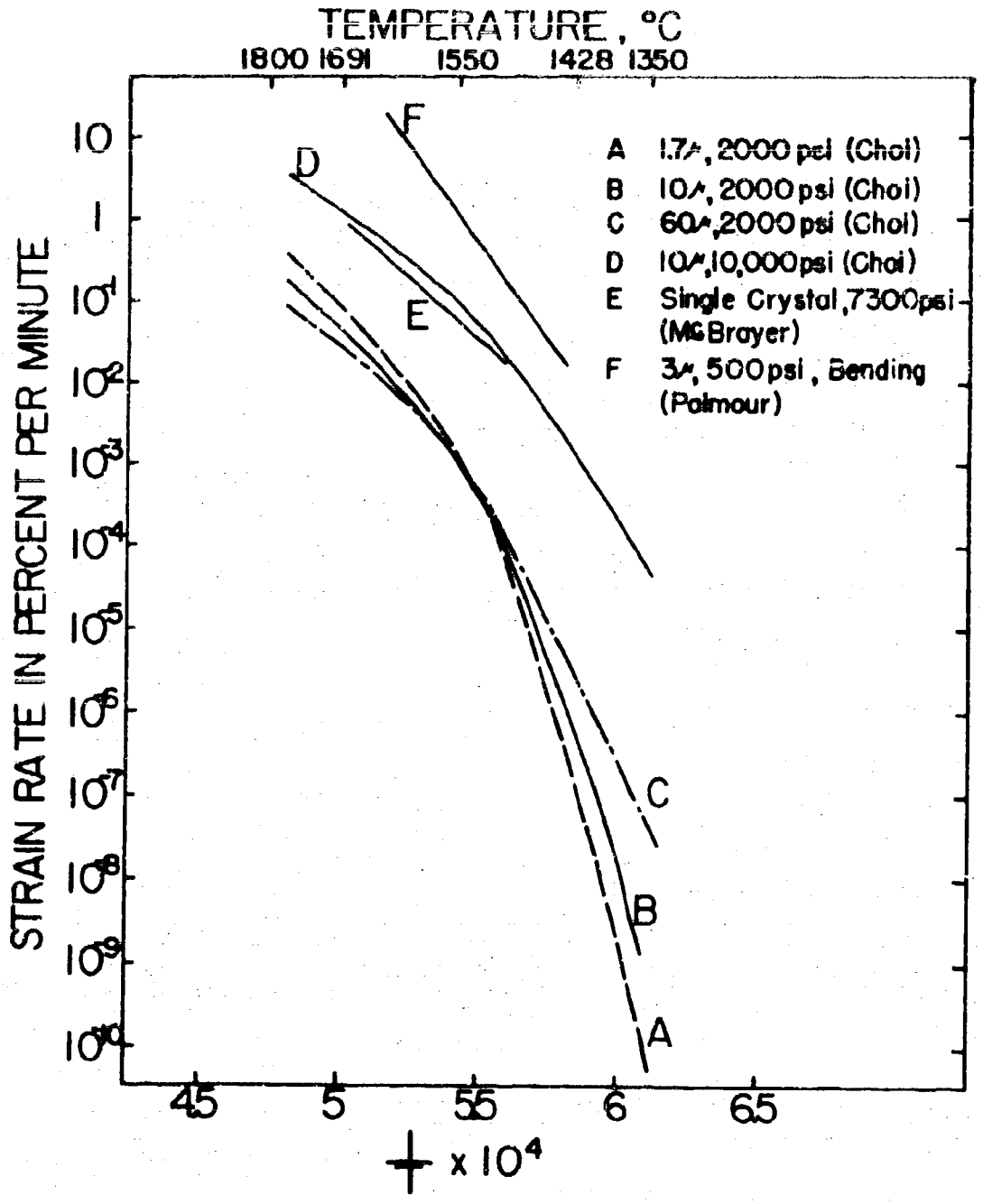

Figure 16. Semi-logarithmic plot of strain-rate computed as a function of reciprocal absolute temperature. Includes comparative data for bending of hot-pressed spinel (after Palmour) and compression testing of alumina rich spinel single crystal (after McBrayer)

interactions. The steep slopes shown by the 2000 psi curves below 1550°C represent extrapolations into strain rate ranges significantly lower than those employed experimentally; at more realistic stress levels for this lower temperature range, e.g., 20,000 psi, the higher temperature strain rates would be heavily extrapolated into strain rate ranges well above those measured experimentally. Such extrapolations may well be misleading, and should not be expected to yield completely realistic kinetic values.

DISCUSSION

The procedure followed in this research for the preparation of specimens is considered reliable because for a given grain size the compressive strengths obtained from many repeated tests under identical conditions agree well and show an acceptably small degree of statistical scatter, generally less than 10% of the mean. The agreement found in these strength data also indicates that the procedure used for compression testing at high temperatures in vacuo is a valid and reproducible one.

The stresses were obtained directly from the load versus time chart on the Instron, but were not corrected for the increase in cross sectional area due to deformation and thermal expansion in the specimen. Thus they must be regarded as engineering estimates of the true stress. However, the flow stresses obtained from the 18 repeated runs for specimens with 10-μ grain size showed that the reproducibility of the test is very high and hence the compression mode of testing of hot-pressed spinel at elevated temperatures is acceptable as a method for studying flow processes in this material.

Accurate measurement of the strain occurring in a specimen at any given moment of testing is difficult partly because of the uncertainty involved in measuring the elastic deformation of the load-transmitting components in the test machine at various stress and temperature levels.

All the principal results have been shown in pictures and graphs in the preceding section. These results point to evidence of work hardening shown by the stress-strain curves and to the development of "wavy" slip markings, recrystallization, and fine transgranular and intergranular cracks in the microstructure in the latter stages of deformation. The kinetics and phenomenology of deformation also have been examined, with particular concern for the significance of strain rate-stress dependence and apparent activation energies.

Evidence of Work Hardening in Stress-Strain Curves

The amount of additional stress necessary to further deform a plastically deforming crystal by a unit amount is called work hardening, and is measured by the slope of the stress-strain diagram above the proportional limit. The principal variations among the stress-strain curves obtained in this experiment are found in 1) the stress level at which the initial flow occurs, 2) the slope of increasing stress with increasing strain above the proportional limit, and 3) the amount of steady-state flow strain. These curves have in common a relatively steep slope in the segment above the proportional limit, indicating a substantial degree of work hardening. This is a predictable result considering that spinel has at least five independent slip systems which von Mises and Taylor consider essential for generalized plastic deformation in a polycrystalline material.

In spinel the dislocations moving along these slip systems are confronted with major structural defects, grain boundaries and sub-grain boundaries, and with opposing dislocations along interpenetrating slip systems, all of which inhibit dislocation movement even after only a small amount of plastic deformation has taken place. The significance of the recurring evidence of work hardening found in the slope of the nonlinear portion of every stress strain curve obtained in this experiment lies in the fact that wherever work hardening occurs plastic deformation has necessarily also occurred.

Work hardening, as is shown by these curves, tends to increase with decreasing grain size, because the total grain boundary area associated with small-grained material is larger than that associated with large-grained material and it is the interference with dislocation movement caused by these major structural defects which produces work hardening. This sensitivity of the work hardening phenomenon to the grain size of the material is demonstrated in the slopes of the plastic portions of typical stress-strain curves obtained in this experiment.

Another influence on the rate and extent of work hardening is the frequency with which dislocations interact with the defects in a crystal. When a large number of dislocations participate in the interaction activity, work hardening is rapid. At elevated temperatures, the generation of new

dislocations from Frank-Read and other sources increases greatly, as does the mobility of the already existing dislocations. As is shown in the stress-strain diagrams, work hardening at high temperatures is substantial, particularly in large grained material where dislocation interactions are favored.

Work hardening is continuously being reduced by a concurrent thermally activated recovery process involving diffusion. Thus, the measured rate of work hardening also depends on how quickly dislocations which have piled up at grain boundaries and other obstacles can be dispersed. This rate depends in turn upon the diffusion rate of vacancies or ions. The diffusion of vacancies to dislocations causes the dislocations to climb out of the pile-ups and to continue to move on the new, less occupied slip plane (Weertman, 1955; Chang, 1963). Vacancy diffusion itself depends on time and temperature. Thus, the slower an external stress is applied, the smaller the work hardening because there is relatively more time for dislocations to disperse or annihilate through some diffusion mechanism. The stress-strain diagrams clearly show the dependence of plastic deformation in hot-pressed spinel upon the plastic strain rate.

As work hardening increases, the deformability of each individual grain continues to decrease. After a certain stress level is reached, and at the point where individual

grains have reached their limit of deformability at that strain rate, the grains begin to translate and rotate as rigid bodies. In this case, the boundaries are forced to open and structural integrity cannot be maintained (Palmour, 1965). Therefore, when the rate at which work hardening in grains still able to deform is equal to the rate at which structural integrity is being lost as grain boundaries open up, a steady-state flow is reached. When this happens the piled-up dislocations further increase the amount of deformation by escaping their barriers through a process of vacancy and ion diffusion. An illustration of this phenomenon may be seen in Figure 7c and d where a large number of fine crack lines have formed in 1.67μ -grained specimens tested at 1428°C as a result of this plastic process. Were it not for this process, the specimen would fail by brittle propagation of Zener or Stroh cracks as soon as the steady-state flow stress was reached. The reason that this 1.67μ specimen has deformed almost one percent at this steady-state region is that work hardening (i.e., plastic flow) continues even while the cracks are developing. These cracks may be designated as ductile cracks, where plastic flow continuously blunts the advancing crack tip, inhibiting its catastrophic propagation.

Microstructure Examination

In attempting to find out exactly in what stage of deformation the fine cracks developed in the specimens with

1.67μ grain size tested at 1428°C, another specimen with the same grain size was tested under identical conditions except that the test was stopped and the load was taken off at approximately fifty percent of the normally observed steady-state flow strain. After testing, it showed a considerably smaller number of fine cracks, suggesting that the majority of such cracks form only after this steady-state condition has been attained. Conversely, generalized deformation of specimens without loss of structural integrity characterizes the region of the stress-strain diagrams preceding the onset of the steady state. The steady state condition observed in these experiments is considered to be equivalent to the third, eventually disruptive, stage of tensile creep observed in ceramic and metallic materials.

The intergranular cracks associated with the slip markings observed in the microstructure of intermediate grained specimens (60μ) in Figure 9 is further evidence that extensive plastic deformation of grains precedes Zener or Stroh-type crack formation along grain boundaries. Stress concentration due to the large number of dislocations piled up at the grain boundary causes intergranular or transgranular fractures. Transgranular crack formation is observed in Figure 11c for 200μ grains, as is apparent grain boundary sliding in Figure 11d. As the local stress increases through dislocation pile-ups, the grain boundary may open as well as slide to accommodate the stress. The crack formed

at the Y-junction of the grains is clearly attributable to plastic deformation as evidenced by the wavy slip lines observed in the adjacent grains.

The small crystallites observed in Figure 9b in pre-existing large grains indicate that recrystallization occurred within these large grains as a result of local strain caused by plastic deformation. It is known that, in metals, polygonization — a process involving climb and glide of dislocations to form small angle boundaries having lower energy than the equivalent number of randomly distributed dislocations — is a necessary preliminary stage to recrystallization. Hence experimental observations of recrystallization denote (a) crystalline plasticity, (b) work hardening due to dislocation interaction with boundaries and other dislocations, and (c) a thermally activated recovery process involving climb of dislocations. An experimental confirmation of dislocation climb and polygonization processes in the spinel structure during high temperature deformation has come from recent dislocation etch pit studies in alumina-rich spinel single crystals. Clear microscopic evidence of polygonization in a specimen loaded in compression along [110] at a strain rate of 10% per minute at 1740°C (and subsequently quench cooled) has been obtained by McBrayer (1965).

The probability of crack formation in the latter stage of deformation depends on the testing temperature, strain rate, and grain size, since cracking is enhanced by the

severity of work hardening, and is made less likely by the availability of an effective recovery process such as dislocation climb and polygonization. Low temperature, high strain rate , and large grain size are favorable conditions for very rapid and severe work hardening, with little likelihood that a recovery process could operate at a sufficient rate to prevent crack initiation. Even though dislocation interactions are responsible for crack initiation under such circumstances, the mobility of dislocations under the locally intense stresses at the advancing crack tip cause its blunting, and thus prevents brittle catastrophic propagation of the cracks.

Choi and Palmour (1964) have discussed the contributions of strain annealing (strain induced grain growth) to dislocations and eventual cracking in polycrystalline spinel repeatedly deformed in compression. They were able to demonstrate by replication fractography that four - and perhaps five - independent sets of interpenetrating slip markings could be microscopically observed in a single large grain ($<200\mu$). In recent high temperature bending experiments (Palmour, 1965), with fine-grained (2-5μ) and dense (approximately 98% of theoretical) hot-pressed spinel of purity comparable with the material used in these studies, the structural integrity of the specimens was still preserved even after 5% of plastic strain at a strain rate of one percent per minute, indicating ductile deformation of spinel; slip markings in the larger grains could be observed microscopically.

Kinetics and Phenomenology of Deformation

Strain Rate-Stress Dependence. The deformation equation (Equation 11) obtained in this research is considerably different from the equations describing creep behavior of other crystalline materials (Zener and Hollomon, 1944; Weertman, 1955). The dependent variable in the present experiment is the flow stress, σ, whereas in the conventional creep test, stress is a constant but independent variable, and strain rate is the dependent one. However, the kinetics involved in the deformation of crystalline material can be compared and discussed with equal facility from either viewpoint.

The n values - which measure the power law relationship between stress and strain rate, ($\dot{\epsilon} \propto \sigma^n$) - obtained in this experiment range from approximately 2 to 7 depending on the testing temperature. These values indicate that the deformation of hot-pressed spinel is achieved by means other than viscous flow, for which process the n value should be unity. The next possible flow mechanism which must be considered is Nabarro-Herring diffusion creep. However, this flow mechanism is categorically ruled out because of the high n values obtained in this experiment (Nabarro-Herring creep is also a viscous process, with n approximately 1) and because the strain rates here employed are almost two orders of magnitude higher than the strain rates under which diffusional creep normally occurs in ceramic materials (Kingery, 1960).

Consequently, the large n values can only be accounted for by a deformation mechanism involving movement of dislocations. Weertman (1955) has shown that for a crystalline material deforming plastically by dislocation movements, and with dislocation climb as the recovery process, the n value should be three to four. The n values obtained in this experiment are in general agreement with the Weertman model.

Apparent Activation Energy. According to the deformation equation obtained in this experiment the contribution attributable to thermal activation is a quadratic function of temperature, $e^{\frac{Q}{RT}(1-\frac{C}{T})}$, rather than the linear Arrhenius-type temperature function, $e^{-Q/RT}$. Thus, when calculated values of $\ln\dot{\epsilon}$ are plotted against the reciprocal of the absolute temperature (Figure 16) the graph is parabolic rather than linear, indicating a progressive change in tangent (apparent activation energy) with change in temperature. The apparent activation energies obtained at temperatures above 1550°C vary from approximately 100 Kcal/mol to about 250 Kcal/mol, in general agreement with the apparent activation energy measured in transverse bending of hot-pressed spinel, approximately 214 Kcal/mol (Palmour, 1965), and in compression testing of single crystals, approximately 130 Kcal/mol (McBrayer, 1965). At very small strain rates, even at low temperatures (where the rate at which ionic or vacancy diffusion can occur is low) grain growth is likely to occur due to the long time required to carry out the tes

The finer the starting grain size, the larger the excess surface energy stored in the boundaries, and the greater the potential for grain growth under given conditions of strain rate and temperature. The small grains grow relatively rapidly, presumably by a strain-annealing process and possibly by some concurrent Nabarro-Herring diffusional process. This grain growth can bring about a large change in the strain rate for a small change in temperature. Thus, the apparent activation energy predicted at temperatures below 1550°C (see Figure 16) is unusally high (approximately 500 Kcal) for very fine grained material (1.67 μ).

At present, diffusion constants and activation energies for self-diffusion of the ionic species in spinel are not available. Thus an unambiguous designation of the deformation mechanism of hot-pressed spinel on the basis of the activation energy alone is impossbile. However, the apparent activation energies obtained in this research are not inconsistent with some thermally activated recovery process involving self-diffusion of a slow moving ionic species, e.g., Oishi and Kingery (1960) reported 185 Kcal/mol as the activation energy for oxygen self diffusion in Al_2O_3, a material closely related to spinel in terms of anion structure, composition, and refractoriness.

SUMMARY AND CONCLUSIONS

Summary

Plastic deformation of dense hot pressed spinel at temperatures above 1350°C is clearly evidenced by the substantial amounts of 1) work hardening shown in the stress-strain curves and 2) steady-state flow strain. The power law strain rate-stress dependence with n ranging from approximately 2 to 7 and apparent activation energies ranging from approximately 100 to 500 Kcal/mol as functions of temperature and grain size are considered to represent the steady state flow process in hot pressed spinel in terms of work hardening on the one hand and some thermally activated recovery process on the other. Limited but direct microscopic evidence for the plasticity of spinel as a result of dislocation movement on multiple slip planes is found in the high incidence of grains containing wavy and straight slip markings and in the large number of recrystallized grains observed in deformed coarse grained material.

Neither the Zener and Hollomon nor the Weertman creep rate equations provided as effective a fit with the experimental data as did the more complex deformation equation reported here. Its temperature interactions with grain size and strain rate, and the quadratic component in the thermal activation term, are highly significant in the statistical sense, and clearly denote an important temperature contribution in addition to a single thermal activation energy. It

is quite probable that two or more different plastic processes are involved with each being rate controlling over a given temperature range. Much additional experimentation would be required to fully resolve each process and its effective range. Both the kinetic data and the microscopic evidence regarding recrystallization and other forms of polygonization tend to support the Weertmen concept of dislocation climb as one of the principal contributing processes to deformation in spinel.

More complete understanding of the role of dislocations in plasticity of spinel might best be sought through the following experimental studies:

1) work with the transmission electron microscope to directly observe the multiple slip systems in spinel and their role in work hardening,
2) fractography studies to reveal the operation of multiple slip systems within grains and to reveal possible occurrences of transgranular slip,
3) kinetic studies conducted over narrower ranges of the experimental variables to delineate possible differences in rate-controlling mechanisms for deformation at different temperatures and grain size levels.

Conclusions

1. Specimens of dense (99^+% of theoretical) hot pressed spinel ranging in grain size from 0.5μ to 200μ deform

plastically at temperatures between 1350°C and 1800°C under dynamic strain rates of 0.05%/min to 5%/min.

2. Work hardening is consistently observed in the stress-strain diagrams obtained in this investigation and the degree of work hardening is strongly dependent on strain rate, temperature, and grain size.
3. The stress at which plastic flow initiates depends largely on the temperature and to a lesser extent on the strain rate and grain size.
4. Wavy slip lines and recrystallization in specimens with intermediate grain sizes are indicative of plastic deformation involving dislocation movements on multiple slip planes.
5. In large grained specimens, localized plastic deformation occurring near grain boundaries and particularly at three-grain intersections induces intergranular and transgranular fractures of Zener and/or Stroh type.
6. When the rate of decrease in strength due to intergranular crack formation is equal to the rate of work hardening, a steady-state flow is reached.
7. Kinetic data and grain boundary sliding observed in some extensively deformed specimens suggest an active participation of the grain boundaries in the latter stage of the deformation process, especially at higher temperatures.
8. Within the ranges of this investigation, the steady state flow stress (ultimate strength) of pure, highly dense polycrystalline spinel can be predicted to within ±5% of

actual values from the deformation equation:

$$\sigma = \left[3.844 \times 10^{-16}\right]\left[d^{2.1382\left(1-\frac{1650}{T}\right)}\right]\left[\dot{\epsilon}^{2.0003\left(1-\frac{1505}{T}\right)}\right]\cdot\left[e^{313,170/RT\left(1-\frac{765}{T}\right)}\right]$$

Where σ = normal steady state flow stress in psi

d = average grain size in microns

$\dot{\epsilon}$ = normal strain rate in percent per minute

R = gas constant

T = temperature in degrees Kelvin

LIST OF REFERENCES

Alper, A. M., McNally, R. N., Ribbe, P. H., and Doman, R. C. 1962. The system $MgO-MgAl_2O_4$. J. Am. Ceram. Soc. 45(6):263-268.

Anderson, H. H. 1952. Magnesium aluminate spinel as a refractory material. Unpublished Ph. D. Thesis, M. I. T., Cambridge. (Microfilm Service, M. I. T.).

Archibald, W. A. and Smith, E. J. D. 1963. Super refractories, pp. 536-591. In A. T. Green and G. H. Stewart (eds.), Ceramics: A Symposium. The British Ceramic Society, London.

Bacon, G. E. 1952. A neutron-diffraction study of magnesium-aluminum oxide. Acta. Crystallogr. 5:684-686.

Box, G. E. P. and Hunter, J. S. 1957. Multifactor experimental designs for exploring response surfaces. Annals Math. Stat. 28(1):195-241.

Bragg, W. H. 1915. The structure of spinel group of crystals. Phil. Mag. 30:305.

Burke, J. E. 1957. Role of grain boundaries in sintering. J. Am. Ceram. Soc. 40(3):80-85.

Carter, R. E. 1961. Mechanism of solid-state reaction between magnesium oxide and aluminum oxide and between magnesium oxide and ferric oxide. J. Am. Ceram. Soc. 44(3):116-120.

Chang, H. C. and Grant, N. J. 1952. Observations of creep of the grain boundary in high purity aluminum. J. Metals 194:619-625.

Chang, H. C. and Grant, N. J. 1953. Grain boundary sliding and migration and intercrystalline failure under creep conditions. J. Metals 5:304-312.

Chang, Roger. 1959. High temperature creep and anelastic phenomena in polycrystalline refractory oxides. J. Nucl. Mater. 1(7):174-181.

Chang, Roger. 1960. Creep of Al_2O_3 single crystals. J. App. Phys. 31:484-487.

Chang, Roger. 1963. Dislocation theories of the high temperature creep of crystalline solids, pp. 275-285. In C. Flingsberg (ed.), Physics and Chemistry of Ceramics. Gordon and Breach, Science Publishers, Inc., New York.

Chen, C. W. and Machlin, E. S. 1957. On a mechanism of high temperature intercrystalline cracking. Trans. AIME 209:829.

Choi, D. M. 1962. Mechanical properties and microstructure of hot-pressed magnesium aluminate. Unpublished Master's thesis, Department of Mineral Industries, North Carolina State College, Raleigh.

Choi, D. M. and Palmour, H. III. 1964. Fractographic evidence of multiple slip in deformed hot-pressed spinel. Presented at the Conference on Role of Grain Boundaries and Surfaces in Ceramics, November 16-18, N. C. State University, Raleigh, N. C. (Submitted for publication in the proceedings).

Choi, D. M., Palmour, H. III, and Kriegel, W. W. 1962. Hot-pressed magnesium aluminate: I. Microstructure and room temperature mechanical properties as described by quadratic multivariable analysis. Presented at 64th annual meeting of American Ceramic Society, Pittsburgh, Pa., May 2. (Submitted to J. Am. Ceram. Soc. for publication).

Clark , F. J. P., Sambell, R. A. J., and Tattersall, H. G. 1962. Cracking at grain boundaries due to dislocation pile-up. Trans. Brit. Ceram. Soc. 61:61-66.

Clark, P. W. and White, J. 1950. Some aspects of sintering. Trans. Brit. Ceram. Soc. 49(7):305-333.

Coble, R. L. 1958. Effect of microstructure on the mechanical properties of ceramic materials, pp. 213-227. In W. D. Kingery (ed.), Ceramic Fabrication Processes. The Technology Press of M. I. T. and John Wiley and Sons, Inc., New York.

Coble, R. L. 1959. Diffusion sintering in solid state, pp. 147-163. In W. D. Kingery (ed.), High Temperature Processes. The Technology Press of M. I. T. and John Wiley and Sons, Inc., New York.

Coble, R. L. and Guerard, Y. H. 1963. Creep of polycrystalline aluminum oxide. J. Am. Ceram. Soc. 46(7):353-354.

Conrad, Hans. 1961. The role of grain boundaries in creep and stress rupture, pp. 218-269. In J. E. Dorn (ed.), Mechanical Behavior of Materials at Elevated Temperatures. McGraw-Hill Book Co., Inc., New York.

Conrad, Hans. 1965. Mechanical behavior of sapphire. J. Am. Ceram. Soc. 48(4):195-201.

Copley, S. M. and Pask, J. A. 1964. Deformation of polycrystalline ceramics. Presented at the Conference on Role of Grain Boundaries and Surfaces in Ceramics, November 16-18, N. C. State University, Raleigh, N. C. (Submitted for publication in the proceedings).

Crandall, W. B., Chung, D. H., and Gray, T. J. 1961. The mechanical properties of ultra-fine hot-pressed alumina, pp. 349-379. In W. W. Kriegel and H. Palmour, III (eds.), Mechanical Properties of Engineering Ceramics. Interscience Publishers, Inc., New York.

Cutler, I. B. 1957. Strength properties of sintered alumina in relation to porosity and grain size. J. Am. Ceram. Soc. 40(1):20-23.

Daniels, A. V., Jr., Lowrie, R. C. Jr., Gibby, R. L., and Cutler, I. B. 1962. Observations on normal grain growth of magnesia and calcia. J. Am. Ceram. Soc. 45(6):282-285.

Davis, M. P. and Palmour, H. III. 1964. Grain boundary sliding in alumina bicrystals. Presented at the Conference on Role of Grain Boundaries and Surfaces in Ceramics, November 16-18, N. C. State University, Raleigh, N. C. (Submitted for publication in the proceedings).

Davis, M. P. and Palmour, H. III. 1965. Mechanical behavior of twist boundaries in alumina bicrystals. Presented in the Symposium on Strengthening Mechanisms in Non-Metallics of the Electrochemical Society, May 10-12, San Francisco, Calif. (Submitted for publication in the symposium).

Folweiler, Robert C. 1961. Creep behavior of pore-free polycrystalline aluminum oxide. J. Appl. Phys. 32(5):773-778.

Fryer, G. M. and Roberts, J. P. 1965. Tensile creep of polycrystalline alumina. Presented at Conference on Mechanical Properties of Non-Metallic Crystals and Polycrystals, April 5-7, University of Birminham, England. Sponsored by Basic Science Section, British Ceramic Society. (Submitted for publication in the proceedings).

Fuerstenau, D. W., Fulrath, R. M., and Pask, J. A. 1961. A fundamental study of the variables associated with the mixing of ceramic raw materials. Quarterly Progress Repts., Nos. 2, 4, and 5. Contract No. AF 33(613)-7763. Wright Air Development Division. Inst. of Engr. Research, University of California, Berkeley, Calif.

Gibbs, P. 1959. Imperfection interactions in aluminum oxide, pp. 21-30. In W. D. Kingery (ed.), Kinetics of High-Temperature Processes. The Technology Press of M. I. T. and John Wiley and Sons, Inc., New York.

Gifkins, R. D. 1956. A mechanism for the formation of intergranular cracks when boundary sliding occurs. Acta Metallurgica 4:98-99.

Gorum, A. E., Parker, E. R. and Pask, J. A. 1958. Effect of surface conditions on room temperature ductility of ionic crystals. J. Am. Ceram. Soc. 41(5):161-164.

Griffith, A. A. 1921. The phenomena of rupture and flow in solids. Phil. Trans. Roy. Soc. (London) 221 A:163-198.

Groves, G. W. and Kelly, A. 1963. Independent slip systems in crystals. Phil. Mag. 8:877-887.

Haertling, G. H. 1964. Hot-pressed lead zirconate-lead titanate ceramics. Presented at 66th Annual Meeting, American Ceramic Society, Chicago, Illinois, April 20. (Submitted to J. Am. Ceram. Soc. for publication).

Herring, C. 1950. Diffusional viscosity of a polycrystalline solid. J. Appl. Phys. 21:423.

Hornstra, J. 1960. Dislocations, stacking faults, and twins in the spinel structure. J. Phys. Chem. Solids 15:311-323.

Hornstra, J. 1963. Dislocations in spinels and related structures, pp. 68-87. In H. H. Stadelmaier and W. W. Austin (eds.), Materials Science Research, Vol. 1. Plenum Press, New York.

Intrater, J. and Machlin, E. S. 1959. Grain boundary sliding and intercrystalline cracking. Acta Met. 7:140-143.

Jackson, J. S. 1961. Hot pressing high-temperature compounds. Powder Met. 8:73-100.

Joffé, A., Kirpitschewa, N. W., and Lewitsky, M. A. 1924. The deformation and strength of crystals. Z. Physik 22:286.

Johnston, T. L., Stokes, R. J., and Li, C. H. 1961. Crack nucleation in magnesium oxide bi-crystals under compression. Thirteenth Technical Rept., Office of Naval Research Project Nonr-2456(00) NR-032-451. Honeywell Research Center, Hopkins, Minnesota.

King, A. G. 1961. The influence of microstructure on the mechanical properties of dense polycrystalline alumina, pp. 333-347. In W. W. Kriegel and H. Palmour III (eds.), Mechanical Properties of Engineering Ceramics. Interscience Publishers, Inc., New York.

Kingery, W. D. 1960. Introduction to Ceramics. John Wiley and Sons, Inc., New York.

Kingery, W. D. and Berg, M. 1955. Study of initial stages of sintering solids by viscous flow, evaporation-condensation, and self-diffusion. J. Appl. Phs. 26:1205-1212.

Kingery, W. D., Francl, J., Coble, R. L., and Vasilos, T. 1954. Thermal conductivity: X, data for several pure oxide materials corrected to zero porosity. J. Am. Ceram. Soc. 37:107-110.

Knudsen, F. P. 1959. Dependence of mechanical strength of brittle polycrystalline specimens on porosity and grain size. J. Am. Ceram. Soc. 42(8):376-387.

Kraus, E. H., Hunt, W. F. and Ramsdell, L. S. 1959. Mineralogy: An Introduction to the Study of Minerals and Crystals. Fifth Edition. McGraw Hill Book Company, Inc., New York.

Kriegel, W. W., Palmour, H. III, and Choi, D. M. 1964. The preparation and mechanical properties of spinel. In P. Popper (ed.), Special Ceramics, 1964: Proceedings of a Conference held at British Ceramic Research Association, Stoke-on-Trent. Academic Press, London. (In press).

Kronberg, M. L. 1955. Polygonization of a plastically bent sapphire crystal. Sci. 122(3170):599-600.

Kronberg, M. L. 1957. Plastic deformation of single crystals of sapphire: basal slip and twinning. Acta Met. 5(9): 507-524.

Kuczynski, G. C., Abernathy, L., and Allan, J. 1959. Sintering mechanism of aluminum oxide, pp. 163-171. In W. D. Kingery (ed.), Kinetics of High-Temperature Processes. The Technology Press of M. I. T. and John Wiley and Sons, Inc., New York.

Mangsen, G. E., Lambertson, W. A., and Best, B. 1960. Hot-pressing of aluminum oxide. J. Am. Ceram. Soc. 43(2): 55-59.

May, J. E. 1959. Polygonization of sapphire, pp. 30-37. In W. D. Kingery (ed.), Kinetics of High-Temperature Processes. The Technology Press of M. I. T. and John Wiley and Sons, Inc., New York.

McBrayer, R. D. 1965. High temperature deformation of alumina-rich spinel single crystal in compression. Unpublished Ph. D. thesis, Department of Mineral Industries, North Carolina State University, Raleigh. (University Microfilm Service, Ann Arbor, Michigan).

McBrayer, R. D., Palmour, H. III, and Mehta, P. K. 1963. Chemical etching of defect structures in alumina-rich spinel single crystals. J. Am. Ceram. Soc. 46(10): 504-505.

Mises, R. von. 1928. Mechanik der plastichen formänderung von kristallen. Zeit. Angew. Math. und Mech. 8:161.

Mott, N. F. 1953. A theory of work-hardening of metals II: flow without slip-lines, recovery and creep. Phil. Mag. 44:742-765.

Nabarro, F. R. N. 1948. Deformation of crystals by motion of single ions, pp. 75-90. Report on a Conference on Strength of Solids. Physical Society of London.

Navias, L. 1961. Preparation and properties of spinel made by vapor transport and diffusion in the system MgO-Al_2O_3. J. Am. Ceram. Soc. 44(9):434-446.

Oishi, Y. and Kingery, W. D. 1960. Self-diffusion of oxygen in single crystal and polycrystalline aluminum oxide. J. Chem. Phys. 33(2):480-486.

Palmour, Hayne III. 1965. Multiple slip processes in magnesium aluminate at high temperatures. Presented at Conference on Mechanical Properties of Non-Metallic Crystals and Polycrystals, April 5-7, University of Birmingham, England. Sponsored by Basic Science Section, British Ceramic Society. (Submitted for publication in the proceedings).

Palmour, Hayne III and Choi, D. M. 1963. Temperature dependence of compressive strength in polycrystalline spinel. Presented at the Spring Meeting of the Southeastern Section, American Ceramic Society, Statesville, N. C. March 23. (Submitted to J. Am. Ceram. Soc. for publication).

Palmour, H. III, Choi, D. M., Barnes, L. D., McBrayer, R. D., and Kriegel, W. W. 1963a. Deformation in hot-pressed polycrystalline spinel, pp. 158-197. In H. H. Stadelmaier and W. W. Austin (eds.), Materials Science Research, Vol I. Plenum Press, New York.

Palmour, Hayne III, Kriegel, W. W., and McBrayer, R. D. 1936b. Research on growth and deformation mechanisms in single crystal spinel. Technical Documentary Report No. ASD-TDR-62-1086. Wright-Patterson Air Force Base, Ohio, Contract No. AF 33(616)-7820. North Carolina State University, Raleigh, N. C.

Palmour, H. III, McBrayer, R. D., Witter, D. E., and Kriegel, W. W. 1964. Growth and deformation mechanisms in single crystal spinel. Technical Documentary Rept. No. ML TDR 64-284. Air Force Systems Command, Wright-Patterson Air Force Base, Ohio. North Carolina State University, Raleigh, N. C.

Parker, E. R. 1961. Ductility of magnesium oxide, pp. 65-87. In W. W. Kriegel and H. Palmour III (eds.), Mechanical Properties of Engineering Ceramics. Interscience Publishers, Inc., New York.

Pratt, P. L. 1964. Plastic deformation in polycrystalline CaF_2. Presented at the Conference on Role of Grain Boundaries and Surfaces in Ceramics, November 16-18, N. C. State University, Raleigh, N.C. (Submitted for publication in the proceedings).

Rankin, G. A. and Merwin, H. E. 1916. The ternary system CaO-Al_2O_3-MgO. J. Am. Ceram. Soc. 38(1):571.

Roy, D. M., Roy, R., and Osborn, E. F. 1953. The system MgO-Al_2O_3-SiO_2 and influence of carbonate and nitrate ions on the phase equilibria. Am. J. Sci. 251(5): 337-361.

Ryschkewitch, E. 1941a. Über die druckfestigkeit einiger keramischer werkstoffe auf der einstoff-basis. Ber. Deut. Keram. Ges. 22(2):54-65.

Ryschkewitch, E. 1941b. Über die zerriesafestigkeit einiger keramischer werkstoffe auf der einstoff-basis. Ber. Deut. Keram. Ges. 22:363-371.

Ryschkewitch, E. 1953. Compression strength of porous sintered alumina and zirconia. J. Am. Ceram. Soc. 32(2):65-68.

Spriggs, R. M., Brissette, L. A., and Vasilos, T. 1964a. Grain growth in fully-dense magnesia. Presented at the 66th Annual Meeting of the American Ceramic Society, Chicago, Illinois, April 21. (Submitted to J. Am. Ceram. Soc. for publication).

Spriggs, R. M., Mitchell, J. B., and Vasilos, T. 1964b. Mechanical properties of pure, dense aluminum oxide as a function of temperature and grain size. J. Am. Ceram. Soc. 47(7):323-327.

Spriggs, R. M. and Vasilos, T. 1963. Effect of grain size on transverse bend strength of alumina and magnesia. J. Am. Ceram. Soc. 46(5):224-228.

Stokes, R. J. 1963. Microstructure and mechanical properties of ceramics. Nineteenth Technical Report. Office of Naval Research Project Nonr-4076(00) NR-032-451. Honeywell Research Center, Hopkins, Minnesota.

Stokes, R. J. and Li, C. H. 1963. Dislocations and strength of polycrystalline ceramics, pp. 133-157. In H. H. Stadelmaier and W. W. Austin (eds.), Materials Science Research, Vol I. Plenum Press, New York.

Stroh, A. N. 1954. The formation of cracks as a result of plastic flow. Proc. Roy. Soc. 223 A:404.

Taylor, G. I. 1938. Plastic strain in metals. J. Inst. Metals 62:307.

Thomas, A. G. and Jones, H. J. 1960. Hot pressing of ceramic powders. Powder Met. 6:160-169.

Tien, T. Y. and Subbarao, E. C. 1963. Grain growth in $Ca_{0.16}Zr_{0.84}O_{1.84}$. J. Am. Ceram. Soc. 46(10):489-492.

Vasilos, T. and Spriggs, R. M. 1963. Pressure sintering: mechanisms and microstructures for alumina and magnesia. J. Am. Ceram. Soc. 46(10):493-496.

Wachtman, J. B. Jr. and Maxwell, L. H. 1954. Plastic deformation of ceramic oxide single crystals. J. Am. Ceram. Soc. 37(7):291-299.

Wachtman, J. B. Jr. and Maxwell, L. H. 1957. Plastic deformation of ceramic single crystals II. J. Am. Ceram. Soc. 40(11):377-385.

Wagner, C. 1936. The mechanism of formation of ionic compounds of higher order (double salts, spinels, silicates). Z. Physik. Chem. 34 B:309.

Warshaw, Stanley I. and Norton, Frederick H. 1962. Deformation behavior of polycrystalline aluminum oxide. J. Am. Ceram. Soc. 45(10):479-486.

Weertman, J. R. 1955. Theory of steady-state creep based on dislocation climb. J. Appl. Phys. 26:1213-1217.

Weertman, J. R. 1957. Steady-state creep through dislocation climb. J. Appl. Phys. 28:362-364.

Westwood, A. R. C. 1961. Fracture of MgO bi-crystals, pp. 89-91. In W. W. Kriegel and H. Palmour, III (eds.), Mechanical Properties of Engineering Ceramics. Interscience Publishers Inc., New York.

Wygant, J. F. 1951. Elastic and flow properties of dense, pure oxide refractories. J. Am. Ceram. Soc. 34(12):374-380.

Zener, C. 1948. Fracturing of metals. Trans. Amer. Soc. Metals 40:3.

Zener, C. and Hollomon, J. H. 1944. Plastic flow and rupture of metals. Trans. ASM 33:163-235.